Title
The Role of Heat-Shock Proteins in Production of Infectious Hepatitis C Viral Particles

Author
Khachatoorian, Ronik

Publication Date
2013

Peer reviewed|Thesis/dissertation

UNIVERSITY OF CALIFORNIA

Los Angeles

The Role of Heat-Shock Proteins in Production of Infectious Hepatitis C Viral Particles

A dissertation submitted in partial satisfaction of the requirements for the degree Doctor of Philosophy in Molecular Biology

By

Ronik Khachatoorian

2013

ABSTRACT OF THE DISSERTATION

The Role of Heat-Shock Proteins

in Production of

Infectious Hepatitis C Viral Particles

by

Ronik Khachatoorian

Doctor of Philosophy in Molecular Biology

University of California, Los Angeles, 2013

Professor Samuel W. French, Chair

We and others have shown nonstructural protein 5A (NS5A) to augment hepatitis C virus (HCV) internal ribosomal entry site (IRES)-mediated translation. We have also co-immunoprecipitated heat shock protein (HSP) 70 with NS5A and demonstrated cellular colocalization leading to the hypothesis that NS5A/HSP70 complex formation is important for IRES-mediated translation. Further, we have shown that the bioflavonoid quercetin, an HSP synthesis inhibitor, and HSP70 knockdown block NS5A-augmentated IRES-mediated translation and infectious virus production. Here, we investigate the mechanisms of antiviral activity of quercetin and six additional bioflavonoids. We demonstrate that catechin, naringenin, and quercetin possess significant antiviral activity, with no associated cytotoxicity. Catechin and

naringenin demonstrated stronger inhibition of infectious virion assembly compared to quercetin. Quercetin markedly blocked viral translation and NS5A-augmented IRES-mediated translation, whereas catechin and naringenin demonstrated mild activity. Moreover, quercetin differentially inhibited HSP70 induction compared to catechin and naringenin. We also identified the NS5A region binding to HSP70 through *in vitro* deletion analyses. Deletion of NS5A domains II and III failed to reduce HSP70 binding, whereas domain I deletion eliminated complex formation. Deletion mapping of domain I identified the C-terminal 34 amino acids (C34) to be the interaction site. C34 expression significantly reduced intracellular viral protein levels and NS5A-augmented IRES-mediated translation, in contrast to same size control peptides from other NS5A domains. Triple-alanine scan mutagenesis identified an exposed beta-sheet hairpin in C34 to be primarily responsible for NS5A-augmented IRES-mediated translation. Moreover, treatment with a 10 amino acid peptide derivative of C34 hairpin suppressed NS5A-augmented IRES-mediated translation and significantly inhibited intracellular viral protein synthesis, with no associated cytotoxicity. We also identified four conserved amino acids in C34 hairpin and showed that altering three of these residues can modulate antiviral activity of the peptides. These results demonstrate the antiviral activity of a number of bioflavonoids, support the hypothesis that the NS5A/HSP70 complex augments viral IRES-mediated translation, and identify a sequence-specific hairpin element in NS5A responsible for complex formation. The peptides corresponding to this hairpin as well as quercetin, catechin, and naringenin are candidates for HCV therapy that target cellular machinery rather than viral proteins reducing the likelihood of viral resistance.

The dissertation of Ronik Khachatoorian is approved.

Asim Dasgupta

David Eisenberg

Ren Sun

Jerome Zack

Samuel W. French, Committee Chair

University of California, Los Angeles

2013

To my family, especially my mother, for their support and help

and

to all people

with hopes that this research will benefit humanity

Table of Contents

Preliminary pages:

Dissertation research:

List of Figures

List of Tables

Abbreviations

APC, allophycocyanin; **ASM**, alanine scan mutagenesis; **C34**, C-terminal 34 amino acids of NS5A domain I; **DMSO**, dimethyl sulfoxide; **FITC**, fluorescein isothiocyanate; **FLuc**, Firefly luciferase; **Fmoc**, 9-fluorenylmethyloxycarbonyl; **GFP**, green fluorescent protein; **GST**, glutathione S-transferase; **HCC**, hepatocellular carcinoma; **HCV**, hepatitis C virus; **HCVcc**, HCV cell culture; **His_6**, hexa-histidine; **HSP**, heat shock protein; **IP**, immunoprecipitation; **IRES**, internal ribosomal entry site; **MALDI-MS**, matrix-assisted laser desorption ionization spectrometry; **NBD**, nucleotide binding domain; **NCR**, non-coding region; **NS**, nonstructural; **NS5A**, nonstructural protein 5A; **ORF**, open reading frame; **PBS**, phosphate-buffered saline; **PCR**, polymerase chain reaction; **PEG-IFN**, pegylated interferon-α; **RLuc**, *Renilla* luciferase; **RP-HPLC**, reverse-phase high performance liquid chromatography; **SBD**, substrate binding domain; **SVR**, sustained virologic response.

Acknowledgements

Special thanks to my family for their continued support throughout the research years. I would also like to thank all the present and past members of the French lab for their contributions to the success of this research. Dr. French has been an excellent mentor throughout my graduate research, and I am grateful to him for the opportunity to conduct research at his lab. I would also like to thank Dr. Nu Lu, Dr. Ekambaram Ganapathy, my undergraduates, Eden Maloney, Yasaman Ahmadieh, Julie Wang, and Edna Miao, former lab manager Oscar Gonzalez, and former lab technician George Yeh. Also thanks to David Dawson and his lab members Michael Arensman and Anna Lay and former lab manger Anne Nguyen Kovochich.

Chapter 1 is a version of: Khachatoorian R, Arumugaswami V, Raychaudhuri S, Yeh GK, Maloney EM, Wang J, Dasgupta A, et al. Divergent antiviral effects of bioflavonoids on the hepatitis C virus life cycle. Virology 2012;433:346-355.

Chapter 3 is a version of: Khachatoorian R, Arumugaswami V, Ruchala P, Raychaudhuri S, Maloney EM, Miao E, Dasgupta A, et al. A cell-permeable hairpin peptide inhibits hepatitis C viral nonstructural protein 5A-mediated translation and virus production. Hepatology 2012;55:1662-1672.

Thanks to my committee members Dr. Asim Dasgupta, Dr. Ren Sun, Dr. Jerome Zack, and Dr. David Eisenberg. Also thanks to Mike Kovochich for helpful discussions, Dr. Charles Rice for providing huh-7.5 cells, and Jeffrey Calimlim and the Flow Cytometry Core Laboratory at UCLA for technical assistance. I am also grateful to our collaborators: the Dasgupta lab, the Sun lab, Dr. Vaithilingaraja Arumugaswami, Dr. Santanu Raychaudhuri, Dr. Piotr Ruchala, Nicole Weatley,

Christopher Sundberg, Dr. Michael Jung, Dr. Xiaolu Cai, Dr. Joseph Loo and Dr. Rachel Loo.

I would also like to acknowledge the sources of funding that made this research possible: R01DK090794 NIH/NIDDK (Samuel French), The Molecular Biology Institute at UCLA, The UCLA Cure Digestive Diseases Research Center, and AI084090 NIH (Asim Dasgupta).

Biographical Sketch

EDUCATION

05/2008 ***B.S., Cell & Molecular Biology (Summa Cum Laude)***
GPA for major: 4.00/4.00 • California State University, Northridge

05/2008 ***B.S., Biotechnology / Medical Technology (Summa Cum Laude)***
GPA for major: 4.00/4.00 • California State University, Northridge

05/2008 ***B.A., English Literature (Summa Cum Laude)***
GPA for major: 4.00/4.00 • California State University, Northridge

PATENT APLLICATION, International

07/05/2011 **French S.W.**, Khachatoorian R., and Ruchala P., *Antiviral Peptides Effective Against Hepatitis C Virus*.

PUBLICATIONS

Epub 10/2012 Khachatoorian R., Dawson D., Maloney E. M., Wang J., French S. W., and **Samuel W. French**, *SAMe Treatment Prevents the Ethanol-Induced Epigenetic Alterations of Genes in the Toll-Like Receptor Pathway*.

06/2012 Lu N., Khachatoorian R., and **Samuel W. French**, *Quercetin: Bioflavonoids As Part of Interferon-Free Hepatitis C Therapy*. Expert Review of Anti-Infective Therapy, 2012. **10**(6):619-21.

Epub 09/2012 Khachatoorian R., Arumugaswami V., Raychaudhuri S., Yeh G. K., Maloney E. M., Wang J., Dasgupta A., and **Samuel W. French**, *Divergent Antiviral Effects of Bioflavonoids on the Hepatitis C Virus Life Cycle*. Virology.

Epub 12/2011 Khachatoorian R., Arumugaswami V., Ruchala P., Raychaudhuri S., Maloney E. M., Miao E., Dasgupta A., and **Samuel W. French**, *A Cell-Permeable Hairpin Peptide Inhibits Hepatitis C Viral Nonstructural Protein 5A-Mediated Translation and Virus Production*. Hepatology, 2012. **55**(6):1662-72.

Epub 03/2008 Paul B., Cloninger C., Felton M., Khachatoorian R., and **Stan Metzenberg**, *A Nonalkaline Method for Isolating Sequencing-Ready Plasmids*. Anal Biochem, 2008. **377**(2): 218-22.

ACADEMIC HONORS

12/2012 Certificate of achievement from the 2012 Seaborg Symposium Student Poster Session. Department of Chemistry and Biochemistry, Jonsson Comprehensive Cancer Center, and David Geffen School of Medicine. University of California, Los Angles.

04/2012 Certificate of achievement for 'Outstanding Research in Experimental Pathology'. Graduate Student Research in Pathology. American Society for Investigative Pathology (ASIP). ASIP Annual Meeting at Experimental Biology 2012. Convention Center. San Diego, CA.

09/2010 'Paul D. Boyer Outstanding Teaching' Award. Molecular Biology Institute. University of California, Los Angeles.

04/2010 Honorable mention. Graduate Research Fellowship Program (GRFP). National Science Foundation (NSF).

06/2008 Scroll of Congratulations, in recognition of my 'Wolfson Scholar' award and valedictorianship. Los Angeles County 5th district supervisor, Michael D. Antonovich and the Board of Supervisors.

ACADEMIC HONORS, CONT.

06/2008 Recognition of my 'Wolfson Scholar' award and valedictorianship. California Assembly Member Paul Krekorian.

06/2008 Valedictorian, class of 2008. California State University, Northridge.

06/2008 'Wolfson Scholar' award (highest honor for graduating seniors). California State University, Northridge. (http://www.csun.edu/notables/khachatoorian)

AWARDS, FELLOWSHIPS, AND GRANTS

12/2012 First Place award in the 2012 Seaborg Symposium Student Poster Session. Department of Chemistry and Biochemistry, Jonsson Comprehensive Cancer Center, and David Geffen School of Medicine. University of California, Los Angles.

2008-2009 'Harvey & Isabelle Kibel' Fellowship. Medical Education and Scholarship Programs. David Geffen School of Medicine. University of California, Los Angeles.

05/2008 'Wolfson Scholar' Scholarship. California State University, Northridge.

2007-2008 'University Scholars' scholarship. California State University, Northridge.

2006-2007 'University Scholars' scholarship. California State University, Northridge.

ORAL PRESENTATIONS

04/22/2012 Khachatoorian R., Arumugaswami V., Ruchala P., Raychaudhuri S., Maloney E. M., Miao E., Dasgupta A., and **Samuel W. French**, *A Cell-Permeable Hairpin Peptide Inhibits Hepatitis C Viral Nonstructural Protein 5A-Mediated Translation and Virus Production*. Graduate Student Research in Pathology. American Society for Investigative Pathology (ASIP). ASIP Annual Meeting at Experimental Biology 2012. San Diego Convention Center.

03/14/2012 Khachatoorian R., Arumugaswami V., Raychaudhuri S., Yeh G. K., Maloney E. M., Wang J., Dasgupta A., and **Samuel W. French**, *Divergent Antiviral Effects of Bioflavonoids on the Hepatitis C Virus Life Cycle*. 2012 Seminar Series. Molecular Biology Institute. University of California, Los Angeles.

02/22/2012 Khachatoorian R., Arumugaswami V., Ruchala P., Raychaudhuri S., Maloney E. M., Miao E., Dasgupta A., and **Samuel W. French**, *A Cell-Permeable Hairpin Peptide Inhibits Hepatitis C Viral Nonstructural Protein 5A-Mediated Translation and Virus Production*. 2012 Seminar Series. Molecular Biology Institute. University of California, Los Angeles.

10/15/2010 Khachatoorian R., Maloney E., Arumugaswami V., Raychaudhuri S., Sun R., Dasgupta A., and **Samuel W. French**, *The Role of Heat-Shock Proteins in Hepatitis C Viral Infection and its Therapeutic Implications*. 2010 MBI Annual Lake Arrowhead Retreat. UCLA Lake Arrowhead Conference Center. Molecular Biology Institute. University of California, Los Angeles.

11/30/2007 Khachatoorian R. and **Stan Metzenberg**, *Expression of Human CRP (C-Reactive Protein) Gene in* Pichia pastoris. 12th Annual Student Research and Creative Works Symposium. California State University, Northridge.

The Role of Heat-Shock Proteins in Production of Infectious Hepatitis C Viral Particles

Introduction

Hepatitis C virus (HCV) infection has a worldwide prevalence of 3% and is the main indication for liver transplantation in developed countries for treatment of cirrhosis[1]. In the United States, HCV is the most common chronic blood borne infection affecting 1.8% of the population and is the major etiologic factor responsible for the recent doubling of hepatocellular carcinoma (HCC) in the United States[2].

Therapy for HCV consists of pegylated interferon-α (PEG-IFN) and ribavirin which is suboptimal as 70-80% of patients in the United States are infected with genotype 1, for which sustained virological response (SVR) is only 50-56%[3]. Generally, therapy of all genotypes can be accompanied by adverse effects, and contraindications to therapy are not infrequent[4]. Former standard antiviral combination therapy with PEG-IFN has been shown to be an effective secondary prevention of HCC[5]; however, 70-80% of HCV patients are not candidates for standard antiviral therapies[6, 7]. Recently, NS3/4A protease inhibitors in combination with PEG-IFN and ribavirin led to an increased SVR, but also increased adverse events including anemia and gastrointestinal symptoms[8]. Nevertheless, a significant number of patients cannot receive these treatments as they require PEG-IFN. Current approaches for preventing HCV-related HCC in patients with contraindications to standard therapy are limited. For these reasons, there is the need to develop adjunct or replacement therapies that are both less toxic and more efficacious in terms of higher SVR and HCC prevention.

HCV is an RNA virus classified in the genus Hepacivirus in the Flavivirus family with a genome composed of a positive sense RNA approximately 10,000 nucleotides in length[9] (Figure 1A). It infects only chimpanzees and humans as well as the Southeast Asian tree shrew tupaia (*Tupaia belangeri*)[10]. The RNA genome lacks a 5' cap for translation and instead relies on an internal ribosomal entry site (IRES) for translation initiation[11]. The entire genome is translated as a single polypeptide approximately 3000 amino acids in length that is subsequently, proteolytically cleaved into 10 viral proteins. These include the structural proteins Core, E1, E2, and the integral membrane ion channel p7, as well as the nonstructural (NS) proteins NS2, NS3, NS4A, NS4B, NS5A and NS5B[12] (Figure 1A). The HCV viral life cycle in a cell can be broken into six phases: 1) binding and internalization, 2) cytoplasmic release and uncoating 3) IRES-mediated translation and polyprotein processing, 4) RNA genome replication, 5) packaging and assembly, and 6) virus morphogenesis and secretion[11] (Figure 2).

The HCV NS5A protein is a 56-59 kDa phosphoprotein that associates with the viral replicase complex. It has been implicated in the regulation of HCV genome replication, IRES-mediated translation of the viral polypeptide, virion assembly, and viral secretion[13-20] (Figure 1B). NS5A also appears to modulate hepatocyte cell signaling by 1) promoting cell survival[21], 2) facilitating the viral life cycle[13-20, 22], and 3) interfering with the hepatocyte innate immune response[23].

The 5' noncoding region (NCR) of the viral genome possesses an IRES[24], a *cis*-acting element found in some host RNA transcripts as well as in viruses that allows ribosomal translation initiation to occur internally within a transcript in lieu of the 5' cap-dependent translation[25]. Under various conditions including heat shock,

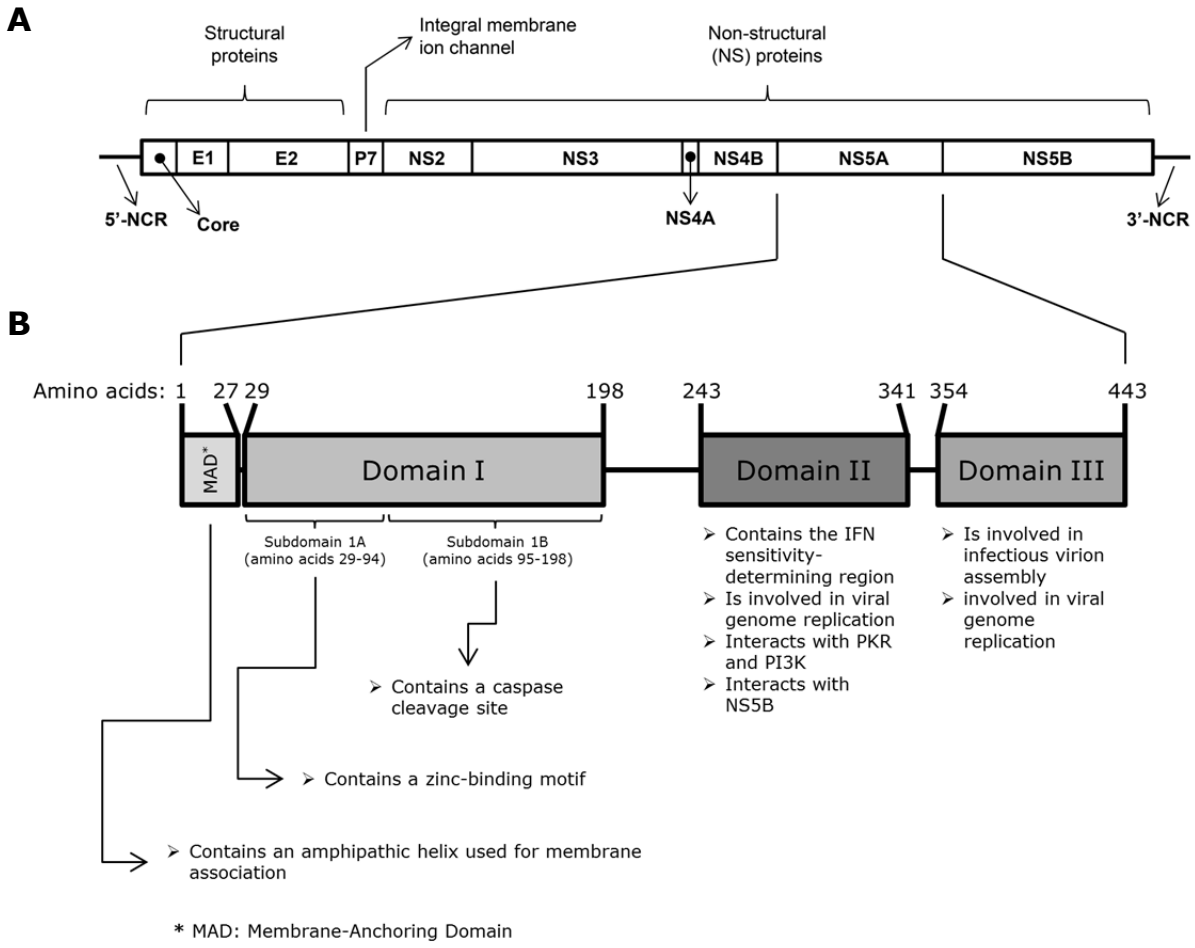

Figure 1. Schematic of the HCV genome (**A**) and NS5A (**B**)

mitosis, hypoxia, differentiation, apoptosis, and infection, general mRNA translation ceases and is replaced with translation of a small subpopulation of mRNAs (usually 3-5%) that is 5' cap independent and IRES dependent[26]. This blocks synthesis of most host proteins and increases levels of specific subgroups of proteins. The role of NS5A in this process is controversial having been shown to stimulate IRES activity by one group and repress activity by another[27, 28].

Interestingly, cellular heat-shock proteins (HSPs) play an important role in the replication of RNA viruses[29-31]. HSPs, which normally assist unfolded or mis-

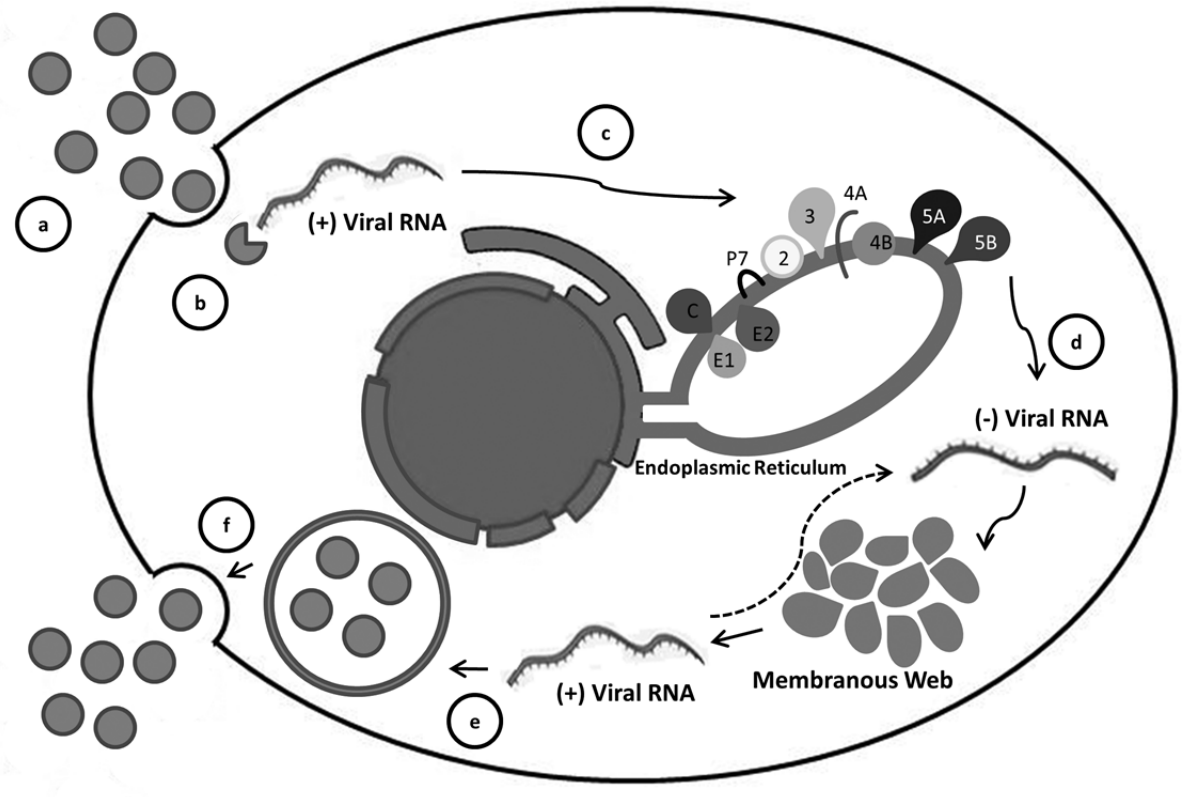

Figure 2. Schematic of HCV life cycle. **A.** Binding and internalization. **B.** cytoplasmic relaese and uncoating. **C.** Viral polyprotein translation and processing. **D.** RNA genome replication. **E.** Packaging and virion assembly. **F.** Virus morphogenesis and secretion. (Adapted from Moradpour et al.[11] and drawn by George K. Yeh.)

folded polypeptide chains to (re)fold into functional proteins, are crucial for cell survival during stressful conditions[32]. We have previously identified, through co-immunoprecipitation, an NS5A/HSP complex composed of NS5A, HSP70, and HSP40 (the cofactor of HSP70) and further shown that virus production is blocked by RNAi-mediated silencing of HSP70 as well as by the HSP synthesis inhibitor quercetin, a bioflavonoid, with no associated cellular toxicity[33]. We have further demonstrated the *in vivo* colocalization of NS5A, HSP70, and HSP40 and have shown that quercetin and RNAi-mediated HSP70 knockdown inhibit NS5A-augmented IRES-mediated translation, as measured by a bicistronic reporter construct which

contains the *Firefly* luciferase and *Renilla* luciferase open reading frames driven by the HCV IRES and a 5' cap, respectively[33]. These findings led to the hypothesis that HCV utilizes an NS5A/HSP complex to facilitate the IRES-mediated translation of its genome.

Bioflavonoids are a group of plant secondary metabolites that serve a variety of functions in plants including pigmentation and resistance to predators. The basic structure of bioflavonoids consists of two phenyl moieties linked together by 3 carbons (Figure 3). A variety of functional groups occur at different positions on this backbone to give rise to the large selection of these naturally occurring compounds. In recent years, bioflavonoids have been extensively studied for their health benefits.

In the first chapter of this dissertation, we report a detailed analysis of the effect of quercetin and a number of other bioflavonoids structurally related to quercetin on viral proliferation and the mechanisms of bioflavonoid-mediated suppression of HCV production. We demonstrate that catechin, naringenin, and quercetin possess significant antiviral activity, with no associated cytotoxicity. Infectious virion secretion was not significantly altered by any of these bioflavonoids. Catechin and naringenin demonstrated stronger inhibition of infectious virion assembly compared to quercetin. In contrast, Quercetin markedly blocked viral translation whereas catechin and naringenin demonstrated mild activity. Similarly quercetin completely blocked NS5A-augmented IRES-mediated translation in the IRES reporter assay, whereas catechin and naringenin had only a mild effect. Moreover, quercetin differentially inhibited HSP70 induction compared to catechin and naringenin.

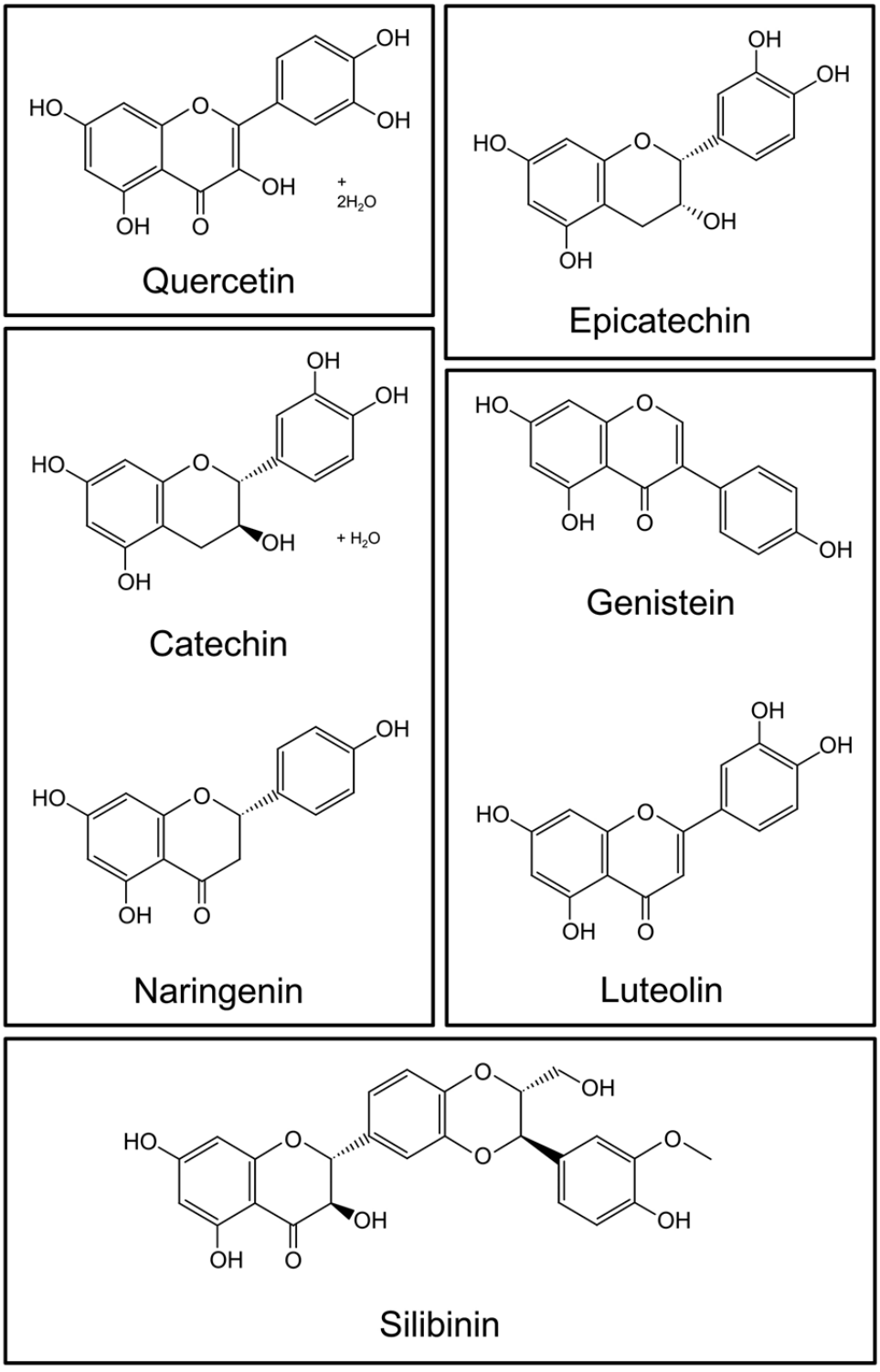

Figure 3. The molecular structure of the bioflavonoids. For naringenin, the structure of the (S) enantiomer is shown; however, the chemical is a racemic mixture of both enantiomers. Silibinin is the major active component of silymarin. (Individual structures were drawn based on the information in Sigma-Aldrich website; catalog numbers are provided in the 'materials and methods' section.)

The second chapter describes the identification of the NS5A/HSP70 interaction site on NS5A. Using recombinant proteins expressed in and extracted from bacteria, we have shown that NS5A and HSP70 directly bind to each other *in vitro*, while minimal interaction with HSP40 was observed. Specific deletion of each of the four NS5A structural elements (membrane-anchoring domain, domain I, domain II, and domain III) revealed that domain I is responsible for HSP70 binding. When each of the three main domains were tested individually, only domain I interacted with HSP70. Fine deletion mapping of domain I demonstrated that the C-terminal 34 amino acids (C34) is necessary for the interaction. Further, addition of this element to domains II and III restored complex formation, indicating C34 to be sufficient for NS5A/HSP70 interaction. In addition, C34 was shown to block NS5A-augmented IRES-mediated translation as well as intracellular viral protein synthesis *in vivo*. Triple alanine scan mutagenesis of C34 revealed the main site of NS5A/HSP70 interaction to be a set of two anti-parallel beta-sheets forming a hairpin that is located near the N-terminus of C34, based on the crystal structure of dimeric NS5A domain I[34]. A 10 amino acid peptide (HCV4) corresponding to this hairpin structure was able to significantly block intracellular viral protein production and IRES-mediated translation even at picomolar concentrations. In addition, deletion mapping of HSP70 identified the N-terminal 41KDa nucleotide-binding domain of HSP70 to interact with NS5A, further validating a sequence-specific NS5A/HSP70 interaction.

Finally, the third chapter reports the identification of the key residues within the C34 hairpin that are involved in the NS5A/HSP70 interaction. We compared the sequence of H77[35] and Con1[34, 35] NS5As and identified four conserved amino acids.

We generated a panel of peptide derivatives of the HCV4 peptide with substitutions at three of these residues and analyzed their efficacy in blocking intracellular viral protein production as above. Substitutions of the three conserved residues affected the potency of the peptide positively or negatively further confirming their role in binding to HSP70. However, substitution of the other non-conserved amino acids with arginines had no effect. While the HCV4 peptide possesses an arginine tag to facilitate cellular entry, incorporation of these arginine residues allowed for generating peptides with no arginine tags that were still capable of penetrating the plasma membrane.

Overall these results indicate that NS5A directly interacts with HSP70, at the C34 hairpin site, to form a complex that seems to be essential for the viral-specific IRES-mediated translation as disruption of this complex by the HCV4 peptide blocks only the IRES-mediated translation and not the 5' cap-dependent translation. This is further supported by the fact that the HCV4 peptide has no toxicity to host cells at concentrations of 1μM and lower. Furthermore, quercetin treatment, which almost completely blocks induction of HSP70, dramatically suppresses viral IRES-mediated translation. RNAi-mediated knockdown of HSP70 displays a similar effect, albeit to a lesser extent[33].

Chapter 1

Divergent Antiviral Effects of Bioflavonoids on the Hepatitis C Virus Life Cycle[36]

We have previously reported that the bioflavonoid quercetin significantly blocks HCV proliferation by inhibiting the NS5A-driven IRES-mediated translation of the viral genome[33]. Also naringenin, another bioflavonoid, has been reported to be able to block viral assembly[37]. Consequently, we sought to determine if a number of other bioflavonoids structurally related to quercetin (Figure 3) would possess antiviral activity and to determine the precise stages of the viral life cycle affected by these compounds.

1.1 Results

We tested a total of seven compounds from a variety of bioflavonoid groups: catechin and epicatechin (flavanols), genistein (an isoflavone), luteolin (a flavone), naringenin (a flavanone), quercetin (a flavonol), and silymarin (a mixture of flavonolignans, where silibinin is the major active component[38]) (Figure 3). Our results demonstrate catechin to possess significant antiviral activity in addition to quercetin and naringenin. Furthermore, we analyzed the effect of these three bioflavonoids on viral translation, infectious virion secretion, and intracellular infectious virion assembly and determined that quercetin is a potent inhibitor of viral translation, while catechin and naringenin are better at blocking viral assembly. None of these compounds affected viral secretion.

1.1.1 Screening of bioflavonoids for cellular toxicity. We first determined the cellular toxicity of these seven compounds at a concentration range of 25-125μM

using standard MTT assays. As shown in Figure 4A, the bioflavonoids can be divided into three groups based on their cytotoxicity profiles. Genistein and luteolin, potential chemotherapeutic agents, display significant cytotoxicity and were not studied further. Naringenin, quercetin, and silymarin possess a cytotoxicity profile similar to the DMSO carrier. Interestingly, catechin and epicatechin result in

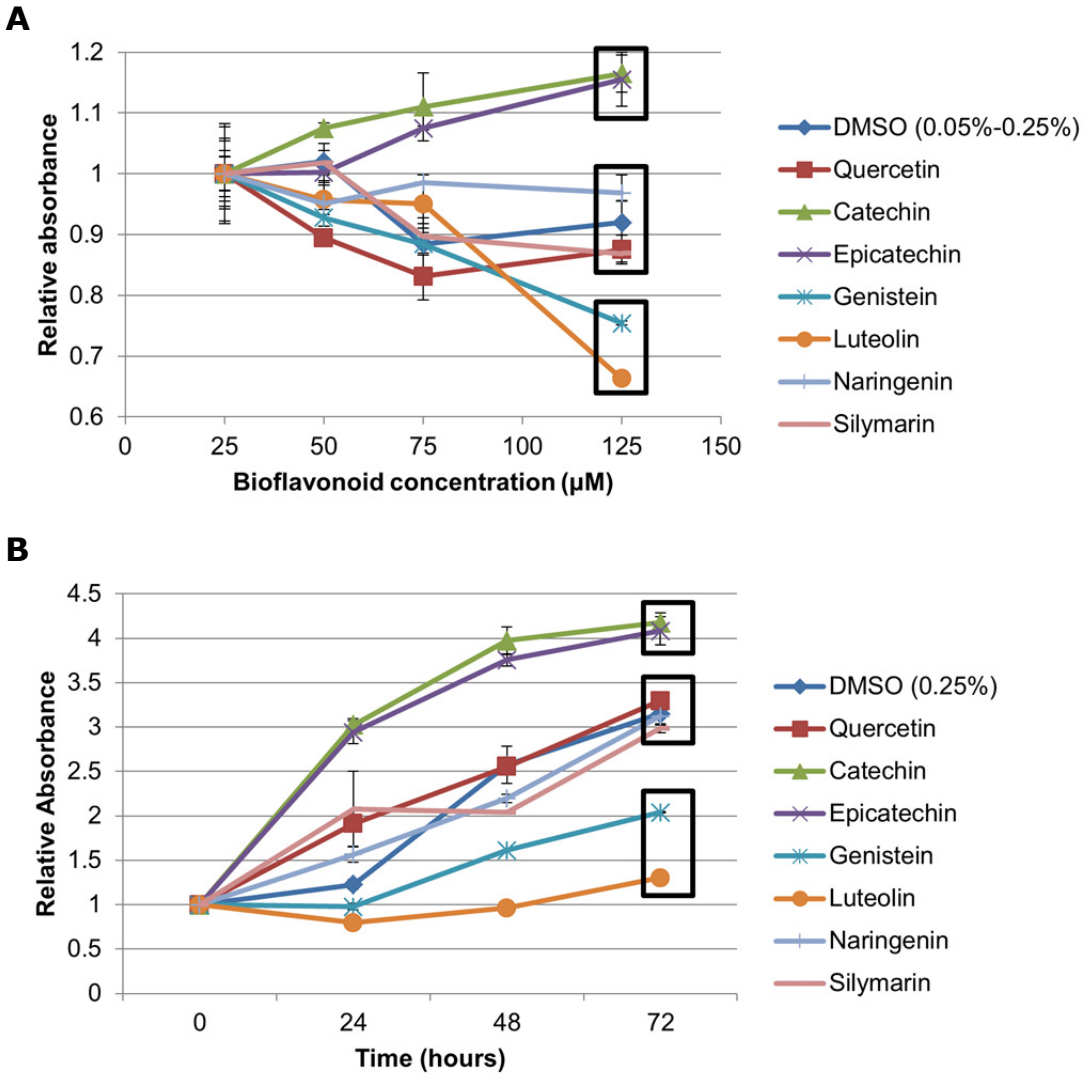

Figure 4. Cytotoxicity of bioflavonoids as determined by MTT assays. **A.** Bioflavonoid cellular toxicity profile in a concentration range of 25-125μM. MTT assays were performed 72 hours post treatment. **B.** Bioflavonoid cellular toxicity profile in a time course of 72 hours at 125μM. All data was normalized to time 0. Boxes indicate flavonoids grouped together based on similar toxicity profiles. (Error bars reflect standard deviation.)

significantly increased absorbance. This may reflect an increase in metabolism, cell division, or cell size; decreased apoptosis; or increased mitochondrial biogenesis. This is a subject of ongoing study. In a separate experiment, we analyzed the toxicity of all bioflavonoids in a time course of 72 hours, and we obtained a similar toxicity profile (Figure 4B).

1.1.2 Catechin, quercetin, and naringenin significantly attenuate HCV production in a dose-dependent manner. Next, we tested the bioflavonoids for their antiviral activity using the HCV cell culture (HCVcc) system measuring intracellular levels of HCV-driven protein expression. Based on our preliminary analyses, we found the concentration range of 25-125μM bioflavonoids to be the most informative for the assays conducted in this study in terms of distinguishing bioflavonoid effects on the stages of viral life cycle. Initially, huh-7.5 cells were infected with the reporter virus and treated with 25μM bioflavonoid for 48 hours, followed by measuring luciferase activity. Quercetin and naringenin displayed significant antiviral activity in agreement with previous reports[33, 37] (Figure 5A). In addition, we found catechin to possess significant antiviral activity as well (Figure 5A). Interestingly, epicatechin, a diastereoisomer of catechin, displayed a slight increase in virus production (Figure 5A). We are currently investigating the opposite effects of catechin and epicatechin on viral proliferation levels. The observed antiviral activities were not indirect effects of bioflavonoids on luciferase expression as determined independently by transfection of a plasmid expressing *Renilla* luciferase (Figure 5B). Silymarin did not result in viral attenuation at 25μM dose (Figure 5A). None of the compounds displayed any cytotoxicity in MTT assays (Figure 5C). We speculated that higher concentrations of silymarin may display

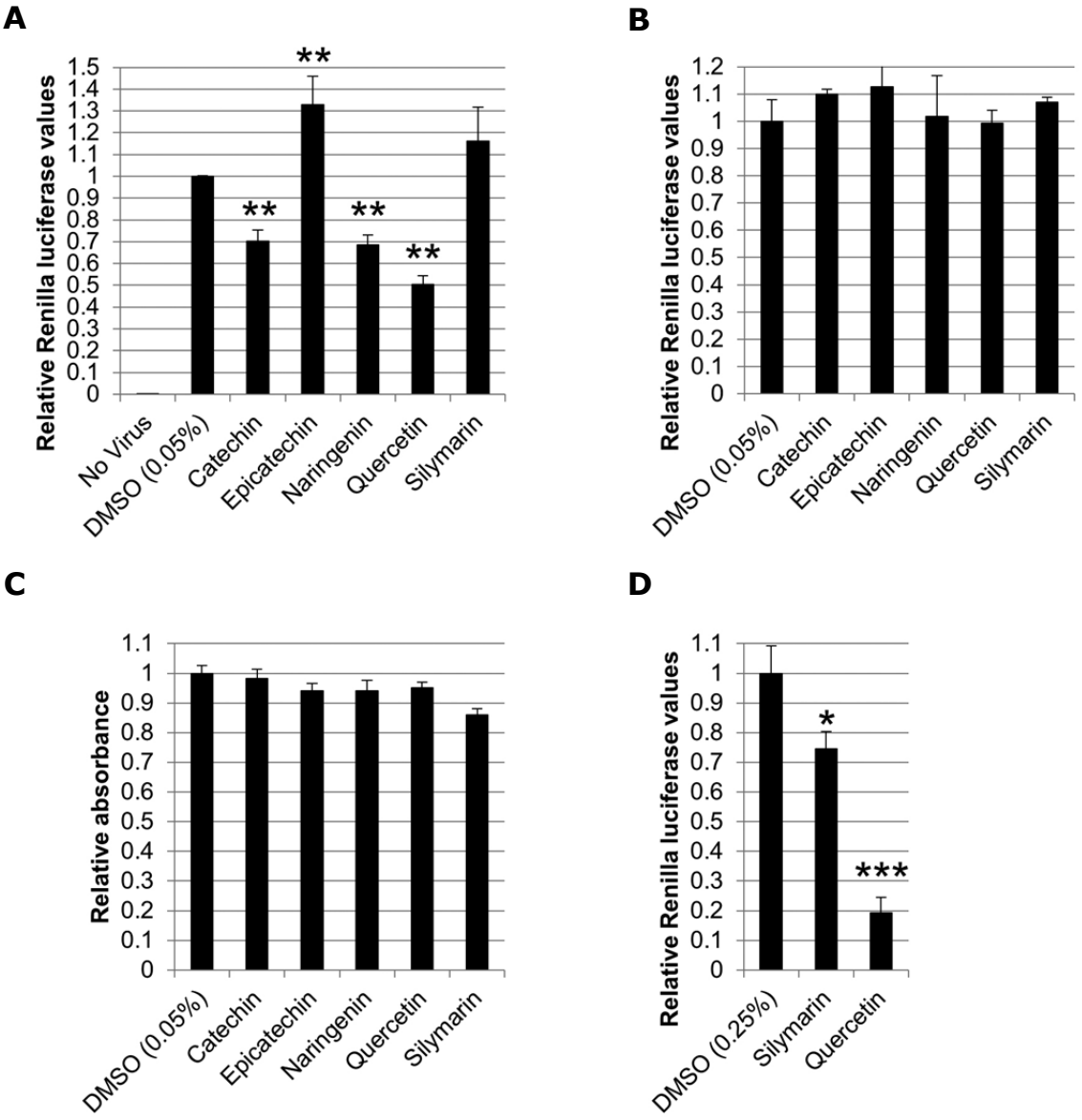

Figure 5. Bioflavonoid antiviral activity. **A.** Effect of 25μM bioflavonoids on viral proliferation. Huh-7.5 cells were infected with the reporter virus and immediately treated with bioflavonoids. 48 hours post treatment, luciferase activity was assayed. **B.** Effect of bioflavonoids on *Renilla* activity. Luciferase assays were performed on cells transfected with pRL-TK plasmid. **C.** MTT assays performed in parallel with assays in parts A and B. **D.** Effect of 125μM silymarin on viral proliferation. Huh-7.5 cells were infected with the reporter virus and treated with bioflavonoids for 48 hours as in part A, followed by luciferase assay. (*, **, and *** indicate $P<0.05$, $P<0.005$, and $P<0.0005$, respectively. Error bars reflect standard deviation.)

some antiviral activity as reported previously[39]. As shown in Figure 5D, 125μM silymarin resulted in a modest antiviral activity in a 48 hour assay. However, silymarin was not studied further due to its significantly lower antiviral activity compared with the other bioflavonoids.

Intracellular viral levels were also determined with a treatment range of 25-125μM catechin, naringenin, and quercetin for 72 hours. All three compounds displayed a dose-dependent antiviral activity with quercetin being the most potent bioflavonoid followed by catechin and naringenin (Figure 6A). To further confirm the antiviral activity of these compounds, the supernatants of these cultures were concentrated 30-fold to remove approximately 97% of bioflavonoids, and the concentrated supernatants were used to infect naïve cells. As shown in Figure 6B, infectious virus production was significantly decreased in a dose-dependent manner.

To further confirm the antiviral activity of catechin, naringenin, and quercetin, huh-7.5 cells were infected and treated with catechin, naringenin, and quercetin for 72 hours as above, followed by measuring viral RNA levels by quantitative reverse transcriptase PCR (qRT-PCR) as well as assaying NS5A protein levels by Western analysis. As shown in Figure 6C and Figure 6D, all three compounds significantly reduced viral RNA and NS5A protein levels, in agreement with the luciferase reporter levels.

1.1.3 Quercetin markedly inhibits intracellular viral protein production compared to catechin and naringenin. We proceeded to determine the mechanism(s) of action of catechin, quercetin, and naringenin, using the HCVcc system. To test the bioflavonoid-mediated inhibition of viral protein production,

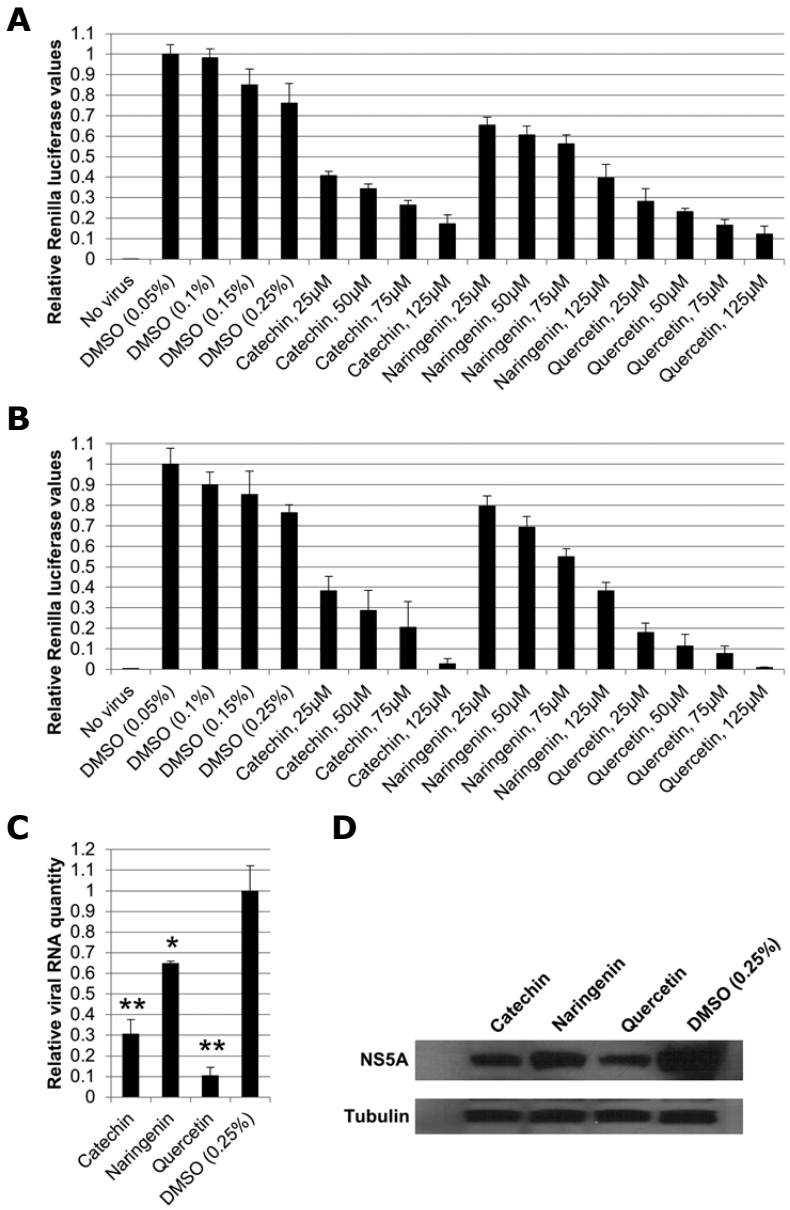

Figure 6. Dose dependent antiviral activity of catechin, naringenin, and quercetin. **A.** Huh-7.5 cells were infected with the *Renilla* reporter virus and immediately treated with a concentration range of 25-125μM of each bioflavonoid for 72 hours, followed by measuring luciferase activity. **B.** Luciferase assays performed on cells infected with the concentrated supernatants of the cells in part A. Huh-7.5 cells were infected with supernatants and harvested 72 hours later. **C.** Bioflavonoid effect on viral genome levels. Huh-7.5 cells were infected with the reporter virus and treated with 125μM bioflavonoid for 72 hours followed by quantitative reverse-transcriptase PCR. **D.** Bioflavonoid effect on viral protein levels. Western analyses for NS5A and loading control tubulin was performed on the same samples from part C. (* and ** indicate $P<0.05$ and $P<0.005$, respectively. Error bars reflect standard deviation.)

huh-7.5 cells were infected and immediately treated with 125μM of bioflavonoid. The 125μM concentration was chosen as it was optimal for distinguishing the mechanism of antiviral activity of the bioflavonoids. Luciferase assays 20 hours after treatment showed that catechin, quercetin, and naringenin significantly inhibited intracellular viral protein translation, with quercetin demonstrating more than two-fold higher activity than catechin and naringenin (Figure 7A). The 20-hour assay time is crucial to limit the assay to one viral life cycle (see below) and eliminate any possible effects of bioflavonoids on other stages of viral life cycle such as virion assembly and secretion.

We also monitored translation levels within 28 hours after infection. As shown in Figure 7B, with no bioflavonoid treatment, viral translation levels steadily increased followed by sharp burst in viral translation between 24 and 28 hour time points. This was interpreted to result from secondary infection. From this we inferred that the viral cycle duration is between 20-24 hours. Bioflavonoid treatment significantly decreased viral protein production during one viral life cycle and afterwards (Figure 7B). Quite interestingly, quercetin, our most potent bioflavonoid, inhibits any increase in viral protein levels during and after one viral life cycle (Figure 7B).

1.1.4 Infectious virion secretion is not inhibited by catechin, naringenin, and quercetin. To determine the effect of bioflavonoids on infectious virion secretion, huh-7.5 cells were infected with the reporter virus. After 24 hours, allowing for sufficient accumulation of intracellular virus, cells were washed to remove secreted virions and treated with 125μM bioflavonoid for 5 hours. This limited time of treatment is necessary to minimize their effect on viral protein

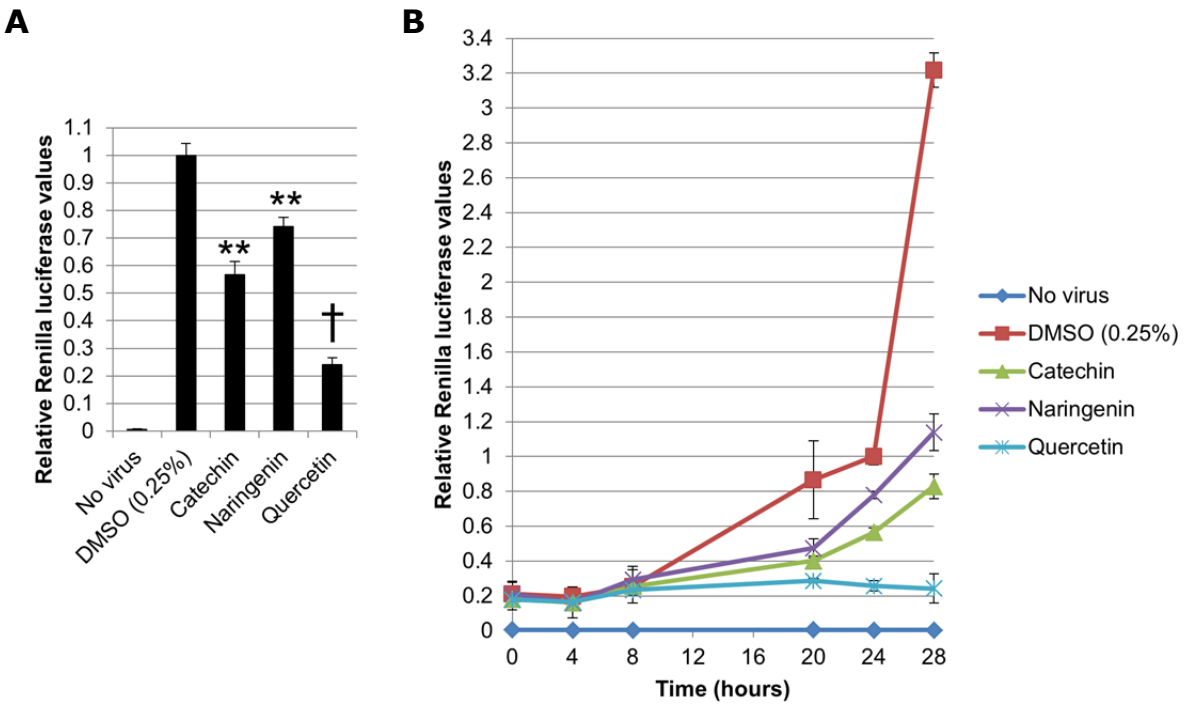

Figure 7. Bioflavonoid effect on intracellular viral protein production. **A.** Huh-7.5 cells were infected with the reporter virus and immediately treated with 125μM bioflavonoid. 20 hours later, luciferase levels were measured. **B.** Luciferase assays performed in a similar way, but at different time points after infection. All values were normalized to the 24 hour time point. (** and † indicate $P<0.005$ and $P<0.000005$, respectively. Error bars reflect standard deviation).

production. Subsequently, supernatants were concentrated 30-fold to remove approximately 97% of bioflavonoids. Elimination of bioflavonoids is necessary to exclude their potential subsequent effects on infection of naïve cells. The concentrated supernatants were used to infect naïve cells. While catechin and quercetin slightly affected viral secretion compared with DMSO, the differences were not statistically significant and may reflect their potent translation inhibitory effects during the 5 hour infection period (Figure 8A). As a positive control, treatment with brefeldin A (BFA), an inhibitor of Golgi-dependent secretion including viral secretion[37], did significantly reduce viral secretion (Figure 8A).

We also ensured that concentrating the culture supernatants indeed removes the bioflavonoids. Aliquots of culture medium were prepared containing 125μM of catechin, naringenin, or quercetin. Two sets of huh-7.5 cells were infected. After the infection period, the supernatants of one set of cells were replaced by the media containing the bioflavonoids as done for all assays in this study. However, for the second set of cells, the medium was subjected to filtration in the same manner as above, and the cleared medium was used to replace the culture supernatants. Luciferase activity was assayed for both sets 48 hours after infection. The filtration

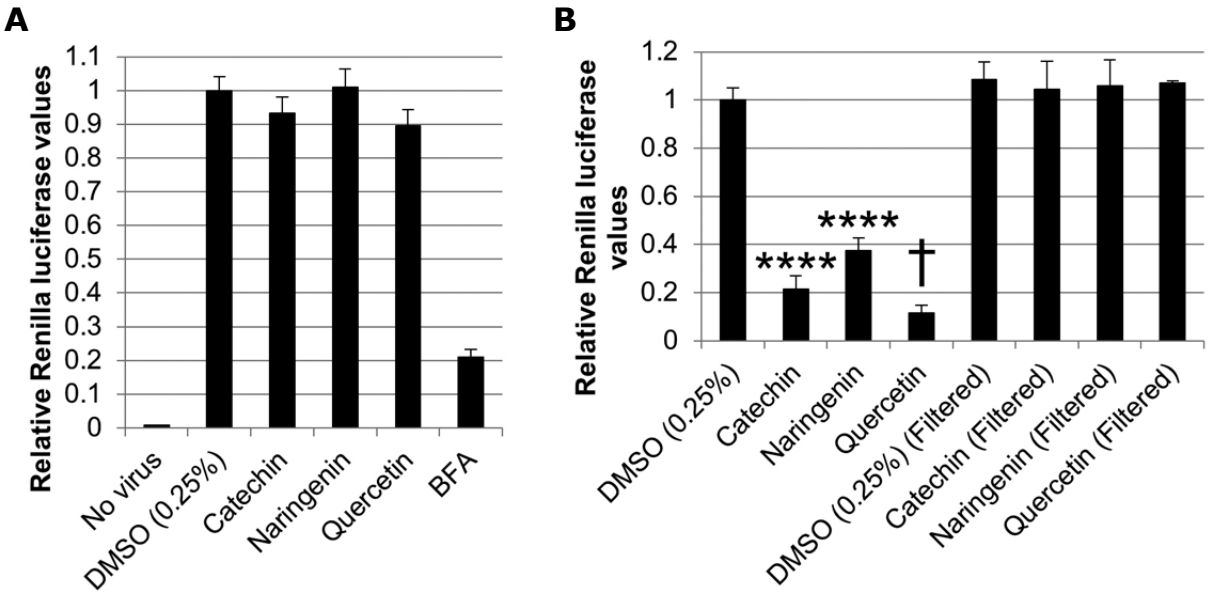

Figure 8. Bioflavonoid effect on infectious virion secretion. **A.** Huh-7.5 cells were infected and 24 hours later, treated with 125μM bioflavonoid for 5 hours. Supernatants were immediately removed and concentrated 30-fold to remove approx. 97% of the bioflavonoids and used to infect naïve cells, followed by luciferase assays 72 hours later. **B.** Control experiment to determine if concentration effectively removed bioflavonoids from supernatants in part A. Two sets of huh-7.5 cells were infected with the reporter virus. Subsequently, the supernatants of one set of cells were replaced with medium containing 125μM bioflavonoid. For the other set of cells, the media containing 125μM bioflavonoid were filtered and concentrated to remove the bioflavonoids. The cleared medium was then used to replace the culture supernatants. 72 hours later, luciferase activity was measured. (**** and † indicate $P<0.00005$ and $P<0.000005$, respectively. Error bars reflect standard deviation.)

step indeed abolished the antiviral activity that was observed with no filtration (Figure 8B).

1.1.5 Catechin, naringenin, and quercetin significantly inhibit intracellular infectious virion assembly. We next determined the effect of bioflavonoids on viral assembly. Two sets of huh-7.5 cells were infected and treated with BFA. One set was used for the assembly assay and the 'control set' for measuring viral translation (below). BFA treatment was performed to trap all assembled virions in the cytoplasm of infected cells. This step is necessary to limit the effect of bioflavonoid treatment to viral assembly alone, as opposed to viral secretion. Three hours later, cells were treated with 125μM bioflavonoids for 5 hours. This limited time of bioflavonoid treatment is necessary to minimize the effect of bioflavonoids on viral protein translation. Supernatants were removed and saved to determine infectious virion production (see below). After adding fresh medium, cells were subjected to three cycles of freeze/thaw to release intracellular virions. The medium was cleared of cellular debris and used to infect naïve cells. As shown in Figure 9A, all three bioflavonoids significantly blocked infectious virion assembly; here catechin and naringenin demonstrated more potency compared to quercetin.

Luciferase assays of the 'control set' of cells showed no significant decrease in viral translation (Figure 9B). BFA inhibition of secretion was verified by infection of naïve cells with the supernatants of the original infection. As shown in Figure 9C, BFA treatment abolished viral secretion as expected, while significant viral secretion occurred when cells were treated with DMSO.

1.1.6 Quercetin blocks NS5A-augmented IRES-mediated translation, whereas naringenin and catechin exhibit mild activity. We tested catechin,

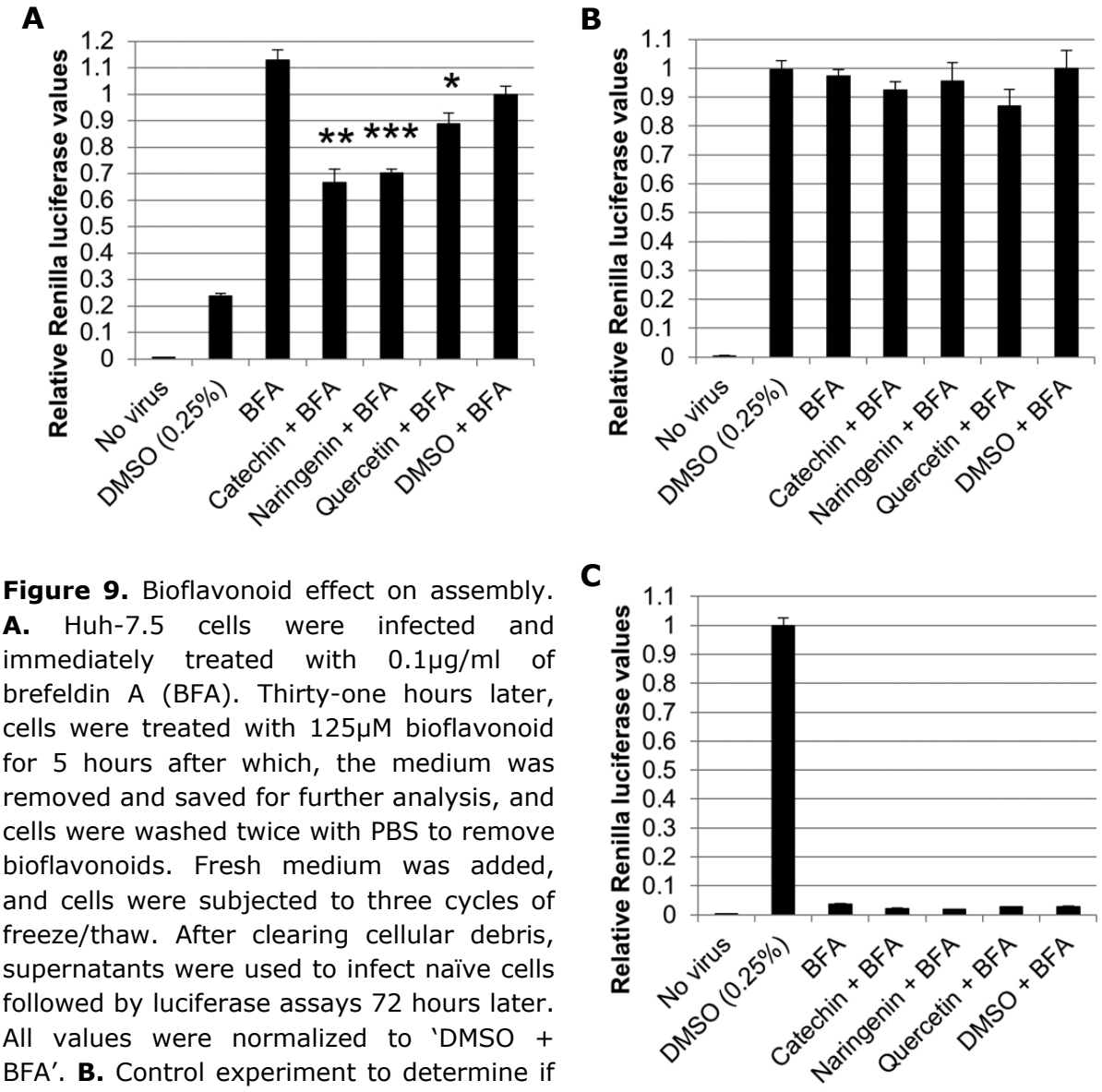

Figure 9. Bioflavonoid effect on assembly. **A.** Huh-7.5 cells were infected and immediately treated with 0.1µg/ml of brefeldin A (BFA). Thirty-one hours later, cells were treated with 125µM bioflavonoid for 5 hours after which, the medium was removed and saved for further analysis, and cells were washed twice with PBS to remove bioflavonoids. Fresh medium was added, and cells were subjected to three cycles of freeze/thaw. After clearing cellular debris, supernatants were used to infect naïve cells followed by luciferase assays 72 hours later. All values were normalized to 'DMSO + BFA'. **B.** Control experiment to determine if bioflavonoids effect viral protein translation in the conditions of part A. Huh-7.5 cells were infected and treated with BFA and bioflavonoids exactly as described in part A. Immediately after the 5-hour bioflavonoid treatment, cells were washed and lysed, and *Renilla* luciferase assay was performed. **C.** Control experiment to determine the effect of BFA on viral secretion in the original part A assembly assay. The supernatants saved from the original culture were concentrated 30-fold to remove bioflavonoids and used to infect naïve cells, followed by luciferase assays 72 hours later. All values were normalized to DMSO treatment. (*, **, and *** indicate $P<0.05$, $P<0.005$, and $P<0.0005$, respectively. Error bars reflect standard deviation.)

naringenin, and quercetin in a previously described cell culture-based bicistronic reporter system to measure levels of viral internal ribosomal entry site (IRES)-

mediated translation[33]. This reporter consists of a *Renilla* luciferase (RLuc) open reading frame (ORF) and a *Firefly* luciferase (FLuc) ORF driven by a 5'-cap and HCV IRES, respectively (Figure 10A). The ratio of *Firefly* to *Renilla* luciferase values (FLuc/RLuc) reflects the levels of HCV IRES-mediated translation. We have previously shown that quercetin suppresses the NS5A-driven increase in IRES-mediated translation[33]. In this study, 293T cells were transfected with the reporter construct and either NS5A or GFP (control) and then treated with 125μM bioflavonoid for 72 hours after which, cells were assayed for dual luciferase activity. All bioflavonoids significantly decreased IRES-mediated translation compared with DMSO (Figure 10B). Quercetin completely blocked NS5A-augmented IRES activity in contrast to catechin and naringenin which demonstrated mild inhibition.

1.1.7 Quercetin strongly inhibits heat shock induced HSP70 expression compered to catechin, naringenin. Quercetin has been reported to inhibit HSP70 expression through different mechanisms[40, 41]. Previously, we have shown HSP70 to form a complex with viral NS5A *in vivo*[33]. Further, as described in chapter 2, we recently showed that the NS5A/HSP70 complex is important for viral protein production *in vivo* and that disruption of this complex through a small peptide inhibitor results in a marked decrease in viral protein synthesis[35]. Based on these observations, we hypothesized that the translation inhibitory effect of quercetin, as well as catechin and naringenin, may be mediated by inhibition of HSP70 expression. To test this hypothesis, huh-7.5 cells were treated with catechin, naringenin, quercetin, or DMSO (control) for 2 hours and subjected to heat shock at 42°C for 30 minutes and allowed to recover at 37°C for 6 hours. Western analysis of cellular lysates with antibody against HSP70 (specifically the HSPA1A isoform

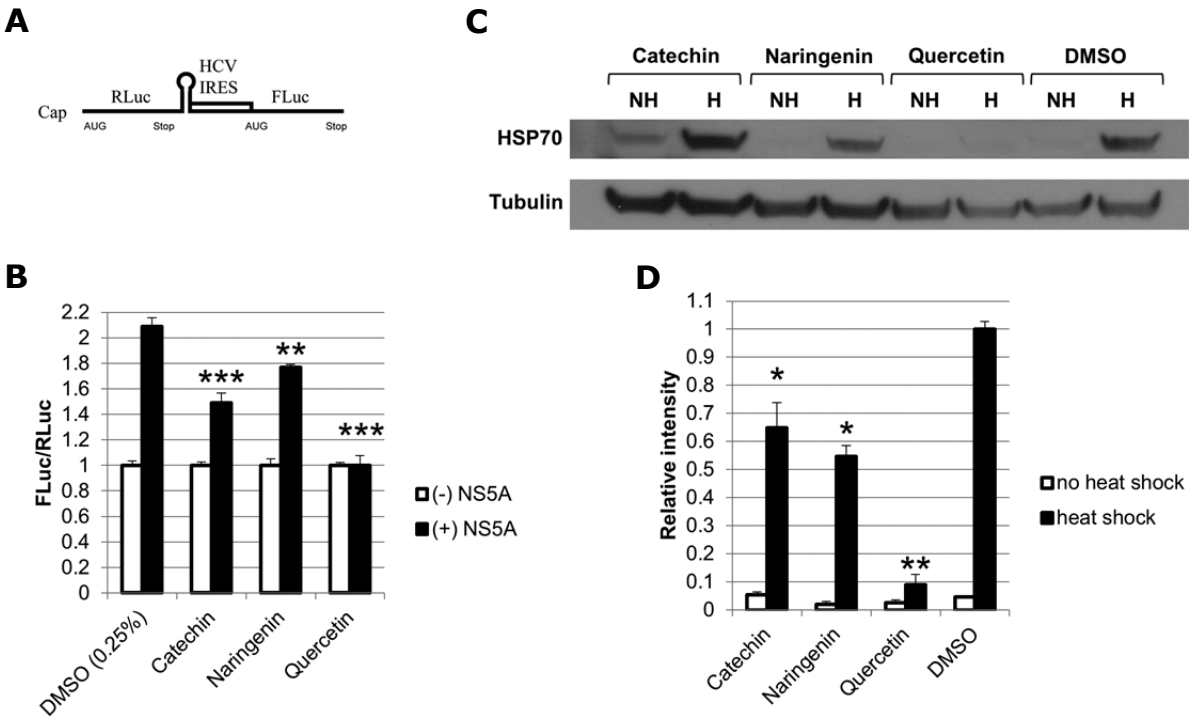

Figure 10. Bioflavonoid effect on IRES-mediated translation. **A.** Schematic of the bicistronic reporter construct used to measure IRES-mediated translation. *Renilla* luciferase (RLuc) and *Firefly* luciferase (FLuc) are driven by a 5' cap and the HCV IRES, respectively. *Firefly* to *Renilla* ratios reflect changes in IRES-mediated translation. **B.** Bioflavonoid effects on IRES-mediated translation. 293T Cells were transfected with the IRES reporter construct and either NS5A or GFP. 12 hours later, cells were treated with 125μM bioflavonoid, followed by luciferase assays 72 hours later. **C.** Western analysis of the effect of bioflavonoids on HSP70 levels after heat shock. Huh-7.5 cells were treated with 125μM bioflavonoids for 2 hours and subjected to heat shock at 42°C for 30 minutes. After 6 hours of recovery at 37°C, cells were lysed, and Western analysis was performed with antibody against HSP70 (HSPA1A). **D.** Densitometry of the Western blot in panel C. HSP70 quantities were normalized to tubulin. (*, **, and *** indicate $P<0.05$, $P<0.005$, and $P<0.0005$, respectively. Error bars reflect standard deviation.)

reported in our previous studies[33, 35]) demonstrated a marked decrease in HSP70 expression in quercetin treated cells (Figure 10C and Figure 10D). A slight decrease in HSP70 was seen for naringenin and catechin treatments (Figure 10C and Figure 10D) consistent with our IRES assay and viral protein production results above (Figure 10B and Figure 7, respectively).

1.2 Discussion

We have previously reported quercetin to efficiently block the NS5A-driven increase in IRES-mediated translation and HCV production[33]. In this study, we further analyzed the mechanisms of action of quercetin and a number of other bioflavonoids structurally related to quercetin.

Initially we tested seven bioflavonoids, including quercetin, for their cellular toxicity, and we found that genistein and luteolin were highly cytotoxic to huh-7.5 cells. Quercetin, naringenin, and silymarin displayed similar toxicity to the DMSO carrier, while catechin and epicatechin had the lowest toxicity and led to a significantly increased absorbance in MTT assays. We conclude that genistein and luteolin are not suitable as anti-HCV treatments due to their significant cytotoxicity at these concentrations.

Next, we screened the remaining five bioflavonoids for their antiviral activity. Catechin, naringenin, and quercetin significantly blocked virus production, while silymarin did not have any effect. Silymarin has previously been shown to inhibit HCV infection in tissue culture primarily through blocking viral entry[39]. We did not see this effect. One possible reason is that we added the compounds after the 3-hour infection time, which would significantly reduce the effect of an entry blocker. Further, the concentration we used was fairly low (25μM). Others have shown approximately 25% reduction in J6/JFH infection (the same backbone as used in this study) when treating at 80 μM[39].

Epicatechin, a diastereoisomer of catechin, led to increased virus production compared with DMSO, and is, therefore, not suitable as an antiviral agent. Recently it was shown that a dimer of catechin and epicatechin can block HCV pseudotype

proliferation[42]. Our finding that catechin and epicatechin have opposite effects on cellular viral levels implies that catechin may be the element in this dimer that displayed antiviral effects. We are currently investigating the opposite effects of catechin and epicatechin on virus production as well as their shared increased absorbance seen in MTT assays. As shown in Figure 3, the dihydrobenzopyran backbone of catechin and epicatechin possesses a dihydroxyphenyl and a hydroxyl group on the pyran moiety. These two groups are oriented differently in three dimensional space; in catechin they are located on the same side of the backbone, while in epicatechin they point in opposite directions. We speculate that the orientation of these side chains may be responsible for the opposite effects of catechin and epicatechin on viral protein translation and are currently investigating this possibility. We have shown previously that viral protein translation is mediated in part by a complex of NS5A and HSP70[33, 35]. Considering our finding that catechin can effect HSP70 expression, it may be possible that the orientation of these side chains determines the effect of catechin and epicatechin on HSP70 expression potentially through their differential interactions with the HSP70 transcription factor.

We chose catechin, naringenin, and quercetin for further analysis because of their antiviral activity. All three bioflavonoids significantly block cellular viral levels in the HCVcc system. Quercetin displays a far more potent effect than catechin and naringenin. Catechin inhibits viral translation more than naringenin, and we speculate that this results in the better long-term viral attenuation by catechin compared with naringenin (Figure 6). We also used the HCV IRES bicistronic reporter assay system to show that the translation inhibitory effect of these

flavonoids are NS5A dependent as there was no change in IRES-mediated translation when GFP was used (instead of NS5A) as a control. This result is consistent with our previous findings on the mechanism of NS5A/HSP70 complex-driven IRES-mediated translation of viral proteins[33, 35].

Intracellular infectious virion assembly is also significantly blocked by catechin and naringenin and to a lesser extent by quercetin. Naringenin has also been previously reported to block virion assembly using a different assay[37]. Infectious virion secretion is not significantly affected by catechin, naringenin (in agreement with a previous report[37]) and quercetin.

Furthermore, we have shown that catechin, naringenin, and quercetin effect induction of HSP70 in cells that are subjected to heat shock. In particular, quercetin has a far stronger inhibitory effect on HSP70 expression. These results support our hypothesis that bioflavonoids mediate their antiviral effects at least in part by blocking heat shock protein (HSP) expression and underscore the role of HSPs in HCV life cycle.

Current HCV treatments are limited and display significant side effect and suboptimal SVR. For these reasons, it is necessary to identify/develop additional antiviral therapies that could be used in place of pegylated interferon-α (PEG-IFN) and ribavirin or as adjunct therapies to increase the SVR. In this study, we have demonstrated the significant antiviral activity of catechin, quercetin and naringenin. Therefore, these bioflavonoids may be candidates for HCV therapy and may be beneficial for patients unable to receive PEG-IFN therapy. Furthermore, because of the different mechanisms of action of these bioflavonoids, combining them may allow for synergistic antiviral activity resulting in better suppression of HCV.

1.3 Materials and Methods

1.3.1 Bioflavonoids. Quercetin (Sigma-Aldrich, 00200595-50MG), catechin (Sigma-Aldrich, C1251-5G), naringenin (Sigma-Aldrich, N5893-1G), epicatechin (Sigma-Aldrich, E4018-5MG), silymarin (Sigma-Aldrich, S0292-10G), genistein (Sigma-Aldrich, G6649-5MG), and luteolin (Sigma-Aldrich, L9283-10MG).

1.3.2 Cell culture. Cell lines huh-7.5 and 293T were maintained in a humidified atmosphere containing 5% CO_2 at 37°C in Dulbecco's Modified Eagle Medium (Mediatech, 10-013-CM) supplemented with 10% fetal bovine serum (Omega Scientific, FB-01) and 2 mM L-glutamine (Invitrogen, 25030). 293T cells were purchased from ATCC (CRL-11268). Huh-7.5 cells were a kind gift from Charles Rice (The Rockefeller University, New York, NY)[43].

1.3.3 Cell viability. Cell viability was determined using MTT Cell Proliferation assay (ATCC, 30-1010K).

1.3.4 Plasmid constructs. The HCV IRES reporter plasmid and the NS5A and GFP retroviral expression vectors pMSCV-NS5A-FLAG and pMSCV-GFP, respectively, have been previously described[33]. An intra-genotype 2 chimeric monocistronic reporter virus virus, pNRLFC based on pJ6/JFH-C parental virus has been described previously[44]. For the current study, we have used a chemically synthesized plasmid pFNX-RLuc (having similar sequences to pNRLFC) for construction of recombinant virus. The pRL-TK (Promega, E2241) plasmid expresses *Renilla* luciferase.

1.3.5 Infectious virus production. pFNX-RLuc was *in vitro* transcribed, and the purified RNA was electroporated into huh-7.5 cells to generate infectious viral supernatant as previously described[44].

1.3.6 Viral assays. All viral assays were done using the HCV reporter virus and with the same titer and multiplicity of infection as described previously[33, 35].

1.3.6.1 Intracellular viral protein production: Huh-7.5 cells were infected for 3 hours, and cells were harvested at the indicated time points. Luciferase activity was measured using the *Renilla* Luciferase Assay System (Promega, E2820).

1.3.6.2 ***Infectious virion secretion:*** The supernatants from the above cultures were concentrated 30-fold by using Amicon Ultra-0.5 mL Centrifugal Filters (Millipore, UFC510096) to remove excess bioflavonoids and used to infect naïve cells for 3 hours. Cells were harvested 72 hours later, and *Renilla* luciferase activity was measured.

1.3.6.3 Intracellular infectious virion assembly: Huh-7.5 cells were infected for 3 hours, and supernatants were removed at indicated time points. Cells were washed with PBS, and fresh medium was added. The cultures were subjected to three cycles of freeze-thaw to release assembled viral particles. These suspensions were cleared of cellular debris and used to infect naïve cells for 3 hours. Subsequently, cells were harvested 72 hours post infection, and luciferase activity was assayed.

1.3.7 Quantitative reverse-transcriptase PCR. Huh-7.5 cells were infected with the *Renilla* reporter virus for 3 hours. Seventy-two hours post infection, cells were harvested, and total RNA was extracted using RNeasy Mini Kit (Qiagen, 74104). cDNA was synthesized using iScript cDNA Synthesis Kit (Bio-Rad, 1708891). qRT-PCR was performed using the Applied Biosystems 7500 Fast Real-Time PCR System with 2x SYBR Green Master Mix (Diagenode, GMO-SG2x-A300) in 25µL reactions. The real-time PCR cycling conditions were 50°C for 2 minutes and 95°C for 10

minutes, followed by 40 cycles at 95°C for 15 seconds, 60°C for 30 seconds, and 72°C for 30 seconds each as well as a final dissociation stage of 95°C for 15 seconds and 60°C for 1 minute. The primers for viral genome were derived from the 5' NCR and were CTGGGTCCTTTCTTGGATAA and CCTATCAGGCAGTACCACA. HCV RNA levels were normalized to the housekeeping gene actin using the primers CCAACCGCGAGAAGATGA and CCAGAGGCGTACAGGGATAG.

1.3.8 IRES reporter assay. 293T cells were treated with 125μM bioflavonoids. Two hours later, cells were transfected with the HCV IRES reporter plasmid and either pMSCV-NS5A-FLAG or pMSCV-GFP. All transfections were done using Fugene6 (Roche, 11814443001). Forty-eight hours post transfection, *Renilla* and *Firefly* luciferase activity were determined using Dual Luciferase Assay System (Promega, E1910).

1.3.9 Antibodies. NS5A (Abcam, ab20342), HSP70 (Santa Cruz Biotech, C92F3A-5), and tubulin (abcam, ab6160).

1.3.10 Densitometry. Western blot images were analyzed by ImageJ v1.45s software according to software instructions.

1.3.11 Statistical analysis. Error bars reflect the standard deviation. P values were determined by student t test.

Chapter 2

A Cell-Permeable Hairpin Peptide Inhibits Hepatitis C Viral Nonstructural Protein 5A-Mediated Translation and Virus Production[35]

We have previously identified, through co-immunoprecipitation, a complex of NS5A and HSPs composed of NS5A, HSP70, and HSP40 (cofactor of HSP70) and demonstrated their colocalization in huh-7 cells[33]. We further showed that both NS5A-augmented IRES-mediated translation and virus production are blocked by HSP70 knockdown as well as by the HSP synthesis inhibitor quercetin, with no associated cytotoxicity[33]. These findings led to the hypothesis that HCV utilizes an NS5A/HSP complex to facilitate IRES-mediated translation of its genome. Therefore, we sought to investigate the binding of NS5A to these HSPs and to characterize the interaction.

2.1 Results

Our results indicate that NS5A binds HSP70 directly, while minimal binding with HSP40 was observed. We identified the site of NS5A/HSP70 interaction on NS5A to be a 10 amino acid hairpin structure at the C terminus of domain I. We further showed that a synthetic peptide corresponding to this hairpin structure potently and dose dependently blocks NS5A-driven IRES-mediated translation and virus production *in vivo*.

2.1.1 The C-terminal region of NS5A domain I is necessary and sufficient for HSP70 binding. We have previously shown that NS5A forms a complex with HSP70 and HSP40 (encoded by HSPA1A and DNAJ2, respectively)[33]. To determine whether NS5A (genotype 1a, clone H77) interacts directly with either or both of

these HSPs, GST-fusion protein pull-down assays were performed using recombinant proteins purified from bacteria. GST-HSP70 interacted with NS5A, while GST-HSP40 showed minimal interaction (Figure 11A). NS5A/HSP70 binding was further confirmed by using GST-NS5A as bait to successfully pull down HSP70 (Figure 11B).

NS5A consists of the four elements: membrane anchoring domain (MAD), domain I, domain II, and domain III (Figure 1B). While MAD is generally considered to be part of domain I, throughout this paper, the term 'domain I' excludes MAD. To determine the individual domain(s) that bind(s) HSP70, each domain was specifically deleted, and the resulting proteins were expressed through *in vitro* coupled transcription/translation reactions. Each deletion mutant was then tested for HSP70 binding using GST pull-down assays with GST-HSP70 as bait. Deletion of NS5A domain I abolished HSP70 binding, while deletion of MAD, domain II, and domain III maintained this interaction (Figure 11C and Figure 11D). Furthermore, NS5A domain I, II, and III were individually expressed *in vitro* and tested for HSP70 binding. Only NS5A domain I bound HSP70 (Figure 11E).

To determine which region of NS5A domain I binds HSP70, N-terminal and C-terminal deletions of domain I were expressed *in vitro* and tested for HSP70 interaction using GST pull-down assays. Deletions of 34 and 68 amino acids at the N terminus of NS5A domain I did not have any effect on its HSP70 binding (Figure 12A). However, deletion of 34 amino acids from the C terminus abolished the HSP70-binding capability of NS5A domain I (Figure 12B). Deleting an additional 34 amino acids at the C terminus showed the same result (Figure 12B).

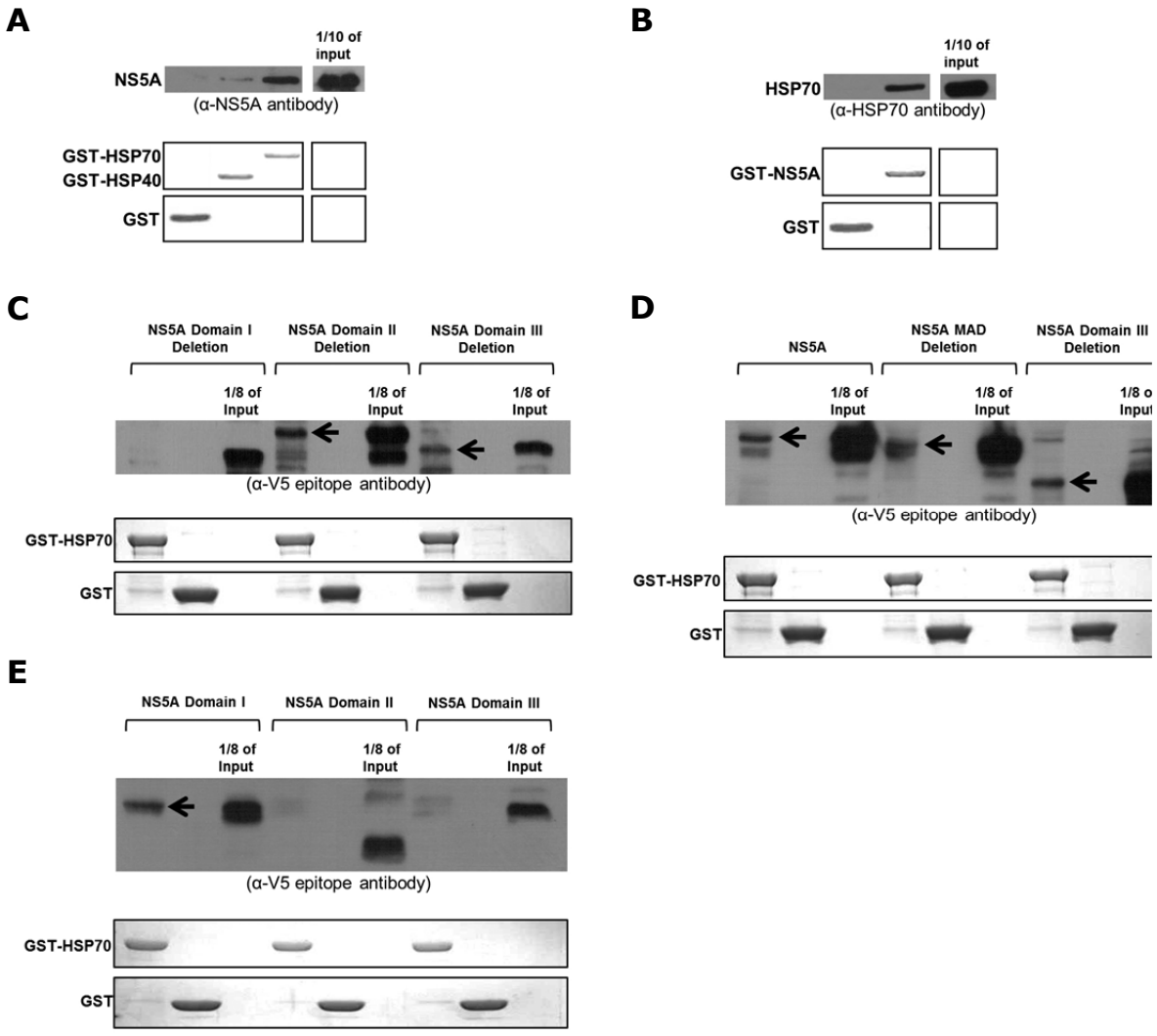

Figure 11. NS5A domain I directly binds HSP70. The upper part of all panels displays Western analysis of GST pull-down targets (antibodies are mentioned underneath). Arrows indicate presence of target polypeptides. The lower part(s) represent(s) Coomassie stains showing GST-fusion bait proteins. **A** and **B.** NS5A directly binds HSP70. **C.** Deletion of NS5A domain I abolishes its HSP70 interaction. **D.** The membrane anchoring domain of NS5A is not required for HSP70 binding. **E.** Only NS5A domain I binds HSP70.

To demonstrate that the C-terminal region of NS5A domain I is indeed responsible for HSP70 binding, the C-terminal 34 amino acids of domain I were added to the NS5A domain I deletion mutant. This addition restored the HSP70 binding capability of NS5A domain I deletion mutant in subsequent GST pull-down

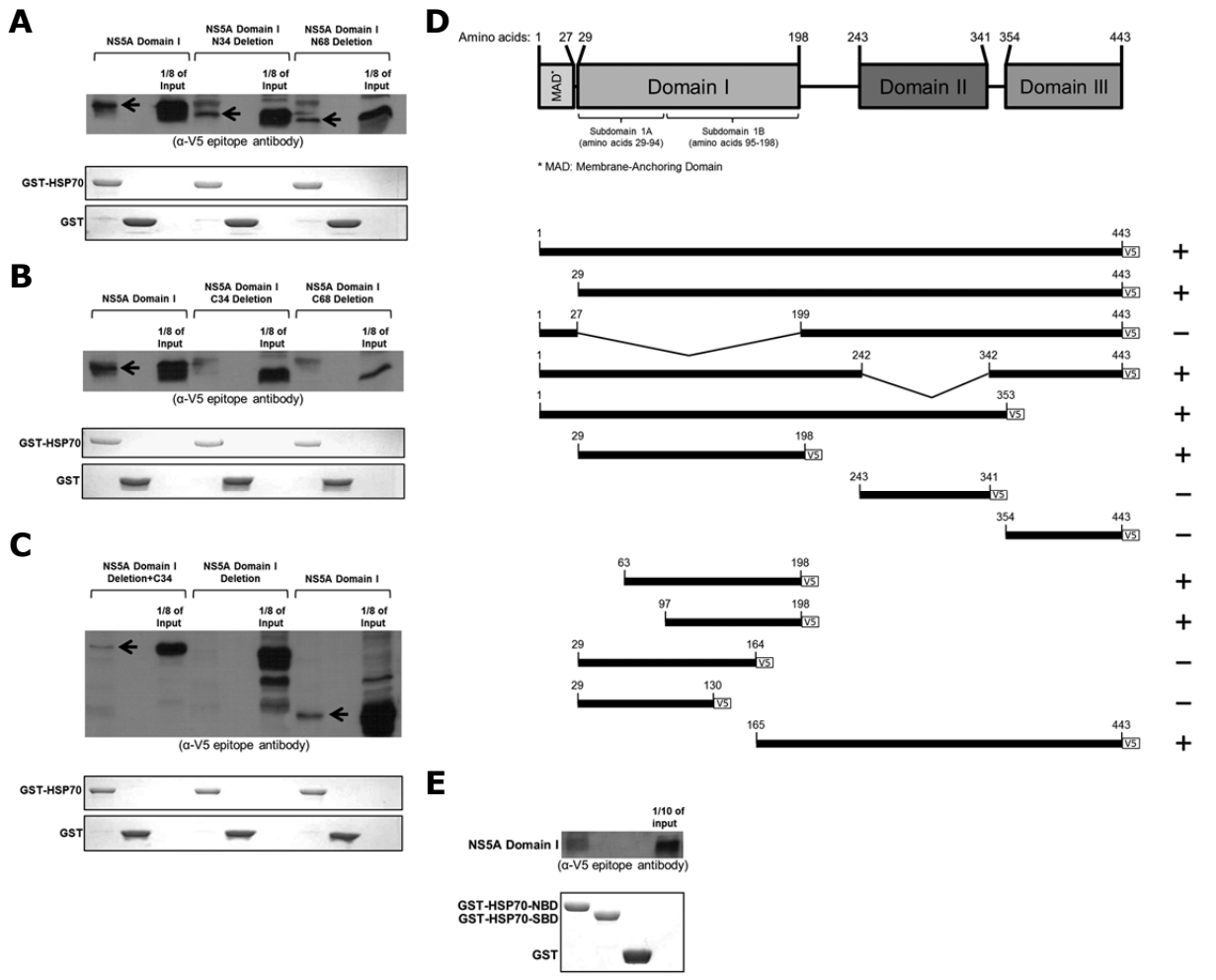

Figure 12. The C-terminal region of NS5A domain I is necessary and sufficient for its interaction with the nucleotide binding domain of HSP70. The upper part of all panels displays Western analysis of GST pull-down targets using antibody against the V5 epitope. Arrows indicate presence of target polypeptides. The lower part(s) represent(s) Coomassie stains showing GST-fusion bait proteins. **A.** The N-terminal region of NS5A domain I is not necessary for HSP70 binding. **B.** The C-terminal 34 amino acids of NS5A domain I (C34) are necessary for HSP70 interaction. **C.** C34 region is sufficient for HSP70 binding. **D.** Summary of all NS5A subclones and GST pull-down analyses reported in Figure 11 and Figure 12. (+) and (-) indicate interaction and lack of interaction with HSP70, respectively. **E.** NS5A domain I directly interacts with the nucleotide binding domain of HSP70, but not with the substrate binding domain.

assays (Figure 12C). The results of all HSP70 binding assays are summarized in Figure 12D.

2.1.2 NS5A directly interacts with the nucleotide binding domain of HSP70. HSP70 binds in a non-specific and sequence-independent manner to hydrophobic peptides through its C-terminal substrate binding domain whereas its N-terminal nucleotide-binding domain (NBD) interacts with regulatory proteins[45]. GST-fusion HSP70-NBD and HSP70-SBD were tested for interaction with NS5A domain I. Only HSP70-NBD interacted with NS5A domain I (Figure 12E).

2.1.3 The C-terminal 34 amino acid peptide of NS5A domain I suppresses NS5A-augmented IRES-mediated translation. After identifying the C-terminal region of NS5A as the HSP70 binding site *in vitro*, we sought to determine whether this region has any functional significance. NS5A is reported to increase IRES-mediated translation in a cell culture-based bicistronic reporter system[27, 33] (Figure 13A). As mentioned in chapter 1, this reporter system consists of a *Firefly* luciferase (ORF) driven by the HCV IRES and a *Renilla* luciferase ORF under the control of a 5' cap (Figure 13A). The ratio of *Firefly* to *Renilla* luciferase activity is used to measure IRES-mediated translation levels.

The C-terminal 34 amino acid peptide corresponding to amino acids 165-198 of NS5A domain I (hereafter referred to as C34) was tested for altering IRES-mediated translation. Peptides of identical length from NS5A domains II and III and a 19 amino acid peptide (P19) from NS3[46] were also tested. C34 was found to block NS5A-augmented IRES-mediated translation in cell culture, while NS5A domain II and III peptides and the NS3 peptide did not (Figure 13B).

All peptides (designed to bear the FLAG tag at their C termini) were determined to be expressed at similar levels through flow cytometry of transfected cells with antibody against the FLAG tag (Figure 13C).

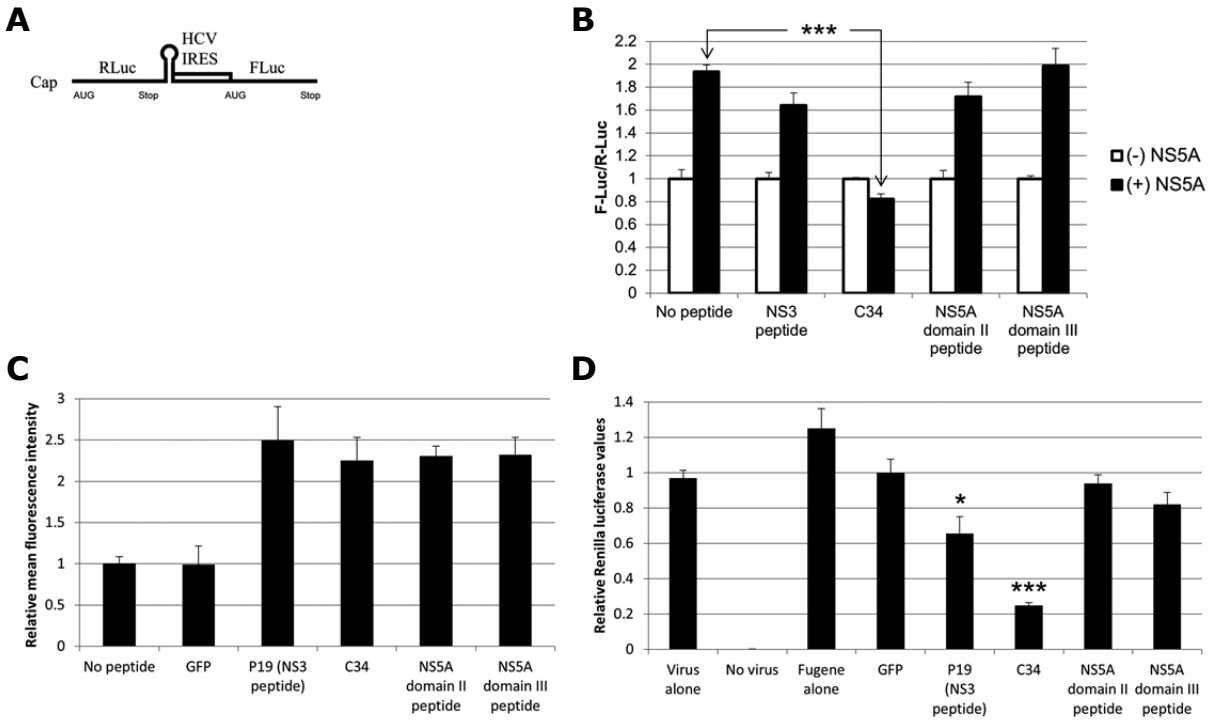

Figure 13. The C-terminal 34 amino acids of NS5A domain I (C34) regulate NS5A-augmented IRES-mediated translation and intracellular viral protein production. **A.** Schematic of the bicistronic reporter construct used to measure IRES-mediated translation. *Firefly* luciferase (FLuc) and *Renilla* luciferase (RLuc) are driven by HCV IRES and a 5' cap, respectively. Each reporter has a stop codon to allow independent expression. *Firefly* to *Renilla* ratios reflect changes in IRES-mediated translation. For all experiments, the IRES reporter, either NS5A or GFP, and a peptide construct (if indicated) were transfected into cells. **B.** C34 suppresses the NS5A-driven increase in IRES-mediated translation. **C.** Flow cytometry of cells transfected with the peptide constructs reveals that all peptides (FLAG-tagged) are expressed at equivalent levels. An allophycocyanin (APC)-conjugated-anti-FLAG antibody was used. **D.** *Renilla* luciferase assay demonstrates that C34 significantly inhibits intracellular viral protein production. Huh-7.5 cells were transfected with the indicated peptide construct and 48 hours later infected with the reporter virus for three hours. Cells were harvested 24 hours post infection, and *Renilla* activity was measured. (* and *** indicate $P<0.05$ and $P<0.0005$, respectively. Error bars reflect standard deviation.)

2.1.4 C34 blocks intracellular viral protein synthesis. Expression of C34 in the HCVcc system using the HCV *Renilla* reporter virus significantly reduced intracellular viral protein production as measured by *Renilla* luciferase reporter activity (Figure 13D). In addition, the P19 peptide from NS3 showed modest reduction in

intracellular virus in agreement with previous studies[46] (Figure 13D). In contrast, expression of equal sized peptides from other areas of NS5A failed to have an effect on infection (Figure 13D). C34 expression had no effect on cell viability as measured by MTT assay (data not shown).

2.1.5 Mutation of an exposed antiparallel beta-sheet hairpin in C34 inhibits the NS5A-driven augmentation of IRES-mediated translation. Scanning triple alanine substitution mutants of C34 were generated to determine the amino acids important for NS5A/HSP70 complex-mediated IRES translation. The IRES reporter, NS5A, and C34 mutants and wild-type were transfected into cells, and IRES activity was measured. The most significant mutations affecting NS5A activity localized to amino acids 171-179 (ASM3, 4, and 5) (Figure 14).

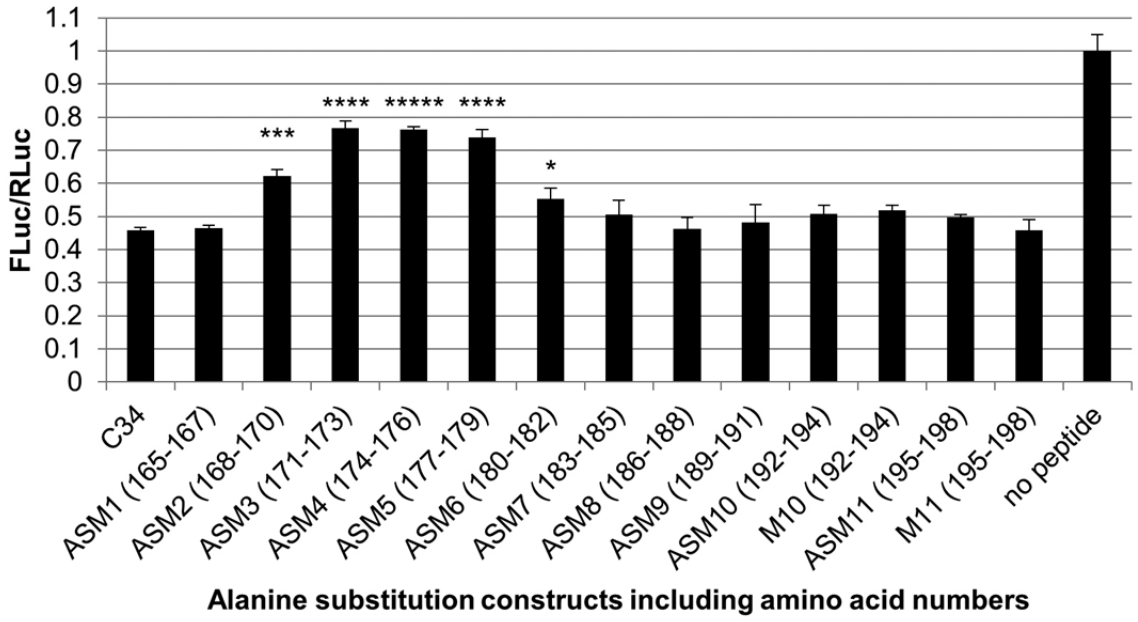

Figure 14. Triple alanine scan mutagenesis (ASM) of the C34 region reveals nine amino acid residues that are critical for IRES-mediated translation. Amino acids 171-179 of NS5A domain I are primarily involved in augmenting IRES-mediated translation. 293T cells were transfected with the indicated C34 mutagenesis construct, the reporter construct (Figure 13A), and NS5A. (*, ***, ****, and ***** indicate $P<0.05$, $P<0.0005$, $P<0.00005$, and $P<0.000005$, respectively. Error bars reflect standard deviation.)

The C34 residues (strain H77) correspond to amino acids 169-202 of the NS5A variant used in the crystal structure of dimeric NS5A domain I[34] (Figure 15A); however, the crystal structure itself terminates at amino acid 198 and, therefore, includes the first 30 amino acids of C34 (Figure 15). Amino acids 171-179 correspond to residues 175-183 of the crystal structure. This region maps to an exposed anti-parallel beta-sheet hairpin (Figure 15B) external to the claw-like structure of NS5A domain I dimer that is proposed to bind single-stranded RNA[34].

2.1.6 Mutations of the C34 hairpin in full-length NS5A impair its ability to augment IRES-mediated translation. To verify the role of C34 hairpin in NS5A-augmented IRES-mediated translation, we introduced mutations in the hairpin region of full-length NS5A. Four triple alanine substitution mutants (corresponding to the ASM3, 4, 5, and 7 constructs) were generated and tested for their effect on IRES-mediated translation. All three mutations in C34 hairpin significantly reduced IRES-mediated translation levels compared to wild-type NS5A (Figure 16). The ASM7 mutation, downstream of the hairpin, however, did not significantly effect IRES-mediated translation (Figure 16).

2.1.7 A ten amino acid peptide corresponding to the C34 hairpin blocks NS5A-augmented IRES-mediated translation. The crystal structure of NS5A domain I reveals the hairpin to be the only moiety in C34 with secondary structure[34] (Figure 15). To determine whether the hairpin alone (as opposed to the entire C34) would be sufficient for IRES activity, a modified peptide of 10 amino acid length corresponding to the C34 hairpin was generated (HCV4 peptide) (Table 1). Two cysteine residues were added to each end to allow for disulfide bond formation and to achieve a conformation similar to the C34 hairpin. An arginine tag

A

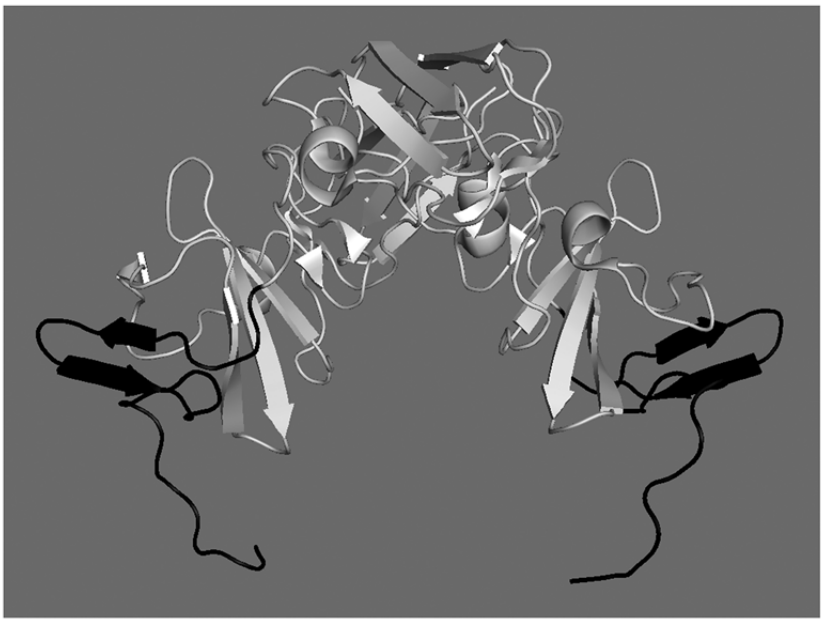

B

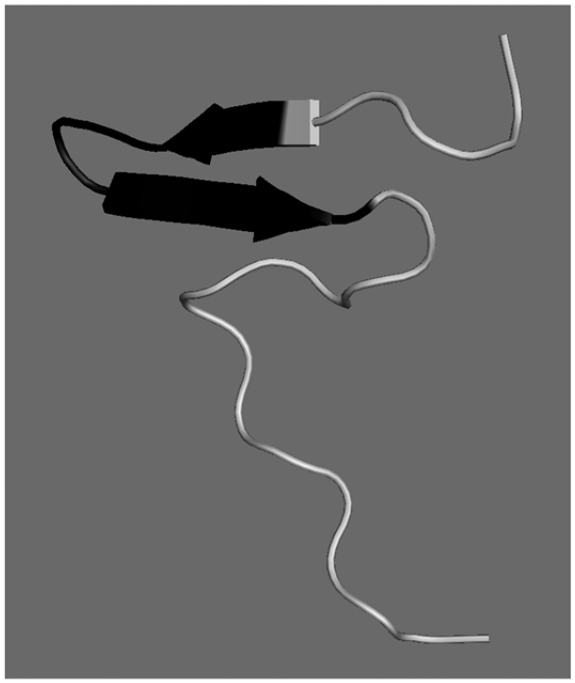

Figure 15. The crystal structure of dimeric NS5A domain I reveals the site of the C34 region and the hairpin within as an exposed secondary structure. **A.** Crystal structure of dimeric NS5A domain I in which the black regions indicate the two C34 regions. **B.** Crystal structure of the C34 region where the black region indicates the hairpin moiety. The panels representing the crystal structure of NS5A domain I and the C34 hairpin were generated by the PyMol software and the '1ZH1' pdb file of dimeric NS5A domain I reported previously[33].

H77 Amino acid position		169	170	171	172	173	174	175	176	177	178	179	180		Cyclization
Crystal structure		Val	Thr	Phe	Leu	Val	Gly	Leu	Asn	Gin	Tyr	Leu	Val		n/a
H77 NS5A		Val	Ser	Phe	Arg	Val	Gly	Leu	His	Glu	Tyr	Pro	Val		n/a
HCV2 peptide		Tyr	Phe	Val	Pro	His	Glu	Ser	Gly	Arg	Val	Val	Leu	$-CONH_2$	No
HCV3 peptide		Cys	Ser	Phe	Arg	Val	(D)Pro	Cha	His	Glu	Tyr	Pro	Cys	$-CONH_2$	-S-S- Bridge
HCV4 peptide	R-(Ahx-R)$_6$-Ahx-Ahx-	Cys	Ser	Phe	Arg	Val	(D)Pro	Cha	His	Glu	Tyr	Pro	Cys	$-CONH_2$	-S-S- Bridge
Arginine tag	R-(Ahx-R)$_6$-Ahx-Ahx-														n/a

Table 1. Characterization of the peptides generated. For more details, refer to Table 2. (Ahx = 6-amino-hexanoic acid; Cha = (L)cyclohexylalanine)

(Table 1) was added to the N-terminal cysteine to allow for efficient uptake by cells without any transfection reagent. MTT assays demonstrated toxicity at 100μM and minimal toxicity at 10μM, while no cytotoxicity was observed at any lower concentrations (Figure 17A). A 48 hour MTT assay was also performed with HCV4, and a similar toxicity profile was obtained (data not shown).

Next, cells were treated with the HCV4 peptide and transfected with the IRES reporter construct and either NS5A or GFP. The peptide blocked NS5A-augmented IRES-mediated translation in a dose dependent manner as shown in Figure 17B.

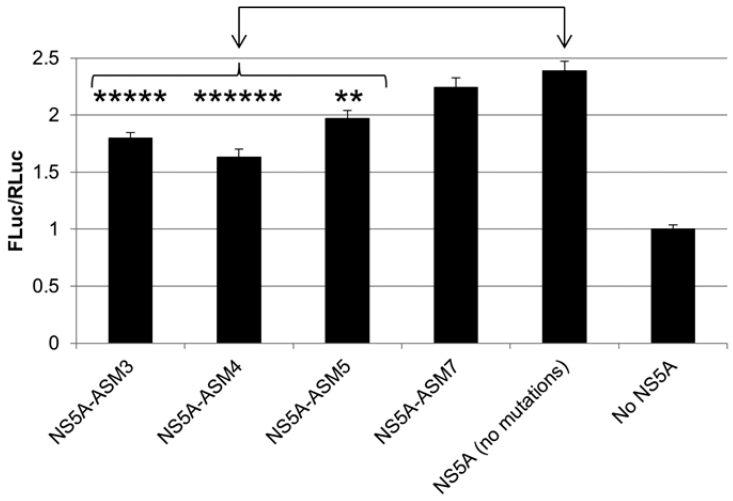

Figure 16. Mutations in NS5A within the C34 hairpin impair the ability of NS5A to augment IRES-mediated translation. 293T cells were transfected with the indicated NS5A mutant and the reporter construct (Figure 13A). (*, *****, and ****** indicate $P<0.05$ and $P<0.000005$, and $P<0.0000005$, respectively. Error bars reflect standard deviation.)

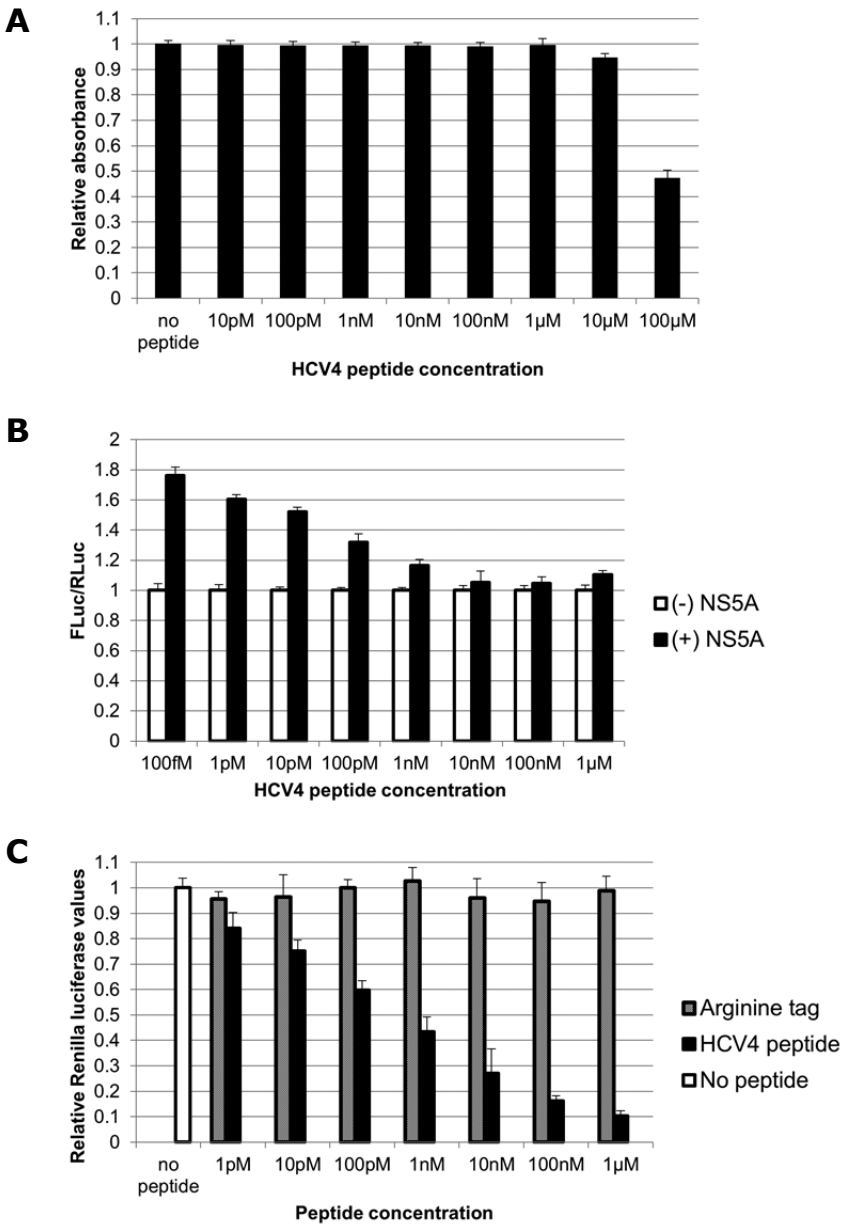

Figure 17. The hairpin structure at the C terminus of NS5A domain I regulates HCV NS5A-driven IRES activity and intracellular virus production. **A.** MTT viability assay showing the cytotoxicity of the HCV4 synthetic peptide derivative of C34 hairpin (Table 1). **B.** HCV4 blocks NS5A-augmented IRES-mediated translation. IRES basal activity in the absence of NS5A was normalized to one for each concentration of peptide. There was a slight decrease in IRES basal activity with increasing peptide treatment (approximately 8% at 1μM). **C.** HCV4 significantly suppresses intracellular viral protein translation. Huh-7.5 cells were treated with the indicated concentrations of HCV4 or the arginine tag control peptide (Table 1) and immediately infected with the *Renilla* reporter virus for three hours. Cells were assayed 24 hours post infection for *Renilla* activity. (Error bars reflect standard deviation.)

2.1.8 The HCV4 peptide blocks intracellular virus production. We next sought to assess the antiviral activity of the HCV4 peptide. Huh-7.5 cells were treated with HCV4 in the HCVcc system and immediately infected with the HCV *Renilla* reporter virus. The HCV4 peptide dramatically suppressed intracellular viral protein production even in picomolar doses, with an estimated IC_{50} of 500pM, while the arginine tag control peptide (Table 1) by itself did not show any effect (Figure 17C). Cellular uptake of the peptide was confirmed by fluorescent microscopy of huh-7.5 cells treated with fluorescein isothiocyanate (FITC)-labeled HCV4 (Figure 18). Further, a non-arginine tagged hairpin peptide (HCV3) (Table 1) transferred into cells using liposomes at 1μM also suppressed viral protein production compared to the sequence-scrambled control peptide (HCV2) (Table 1) (Figure 19).

We further hypothesized that the potent translation inhibitory effect of HCV4 should also result in a significant inhibition of infectious virion secretion and viral RNA replication. Levels of infectious virion secretion were measured by infecting naïve huh-7.5 cells with the supernatant of infected cells. Figure 20A shows that viral secretion is blocked with HCV4 treatment. Furthermore, qRT-PCR analysis of HCV4-treated cells revealed a significant decrease in viral RNA replication levels (Figure 20B).

***2.1.9 The HCV4 peptide blocks NS5A/HSP70 complex formation* in vitro *and binds to HSP70* in vivo.** To determine if disruption of the NS5A/HSP70 complex is the mechanism by which the C34 hairpin might inhibit IRES activity and virus production, we tested the ability of the HCV4 peptide to block NS5A/HSP70 complex formation *in vitro*. GST pull-down assays were performed as before using GST-HSP70 as bait and NS5A domain I. Increasing concentrations of HCV4 was able

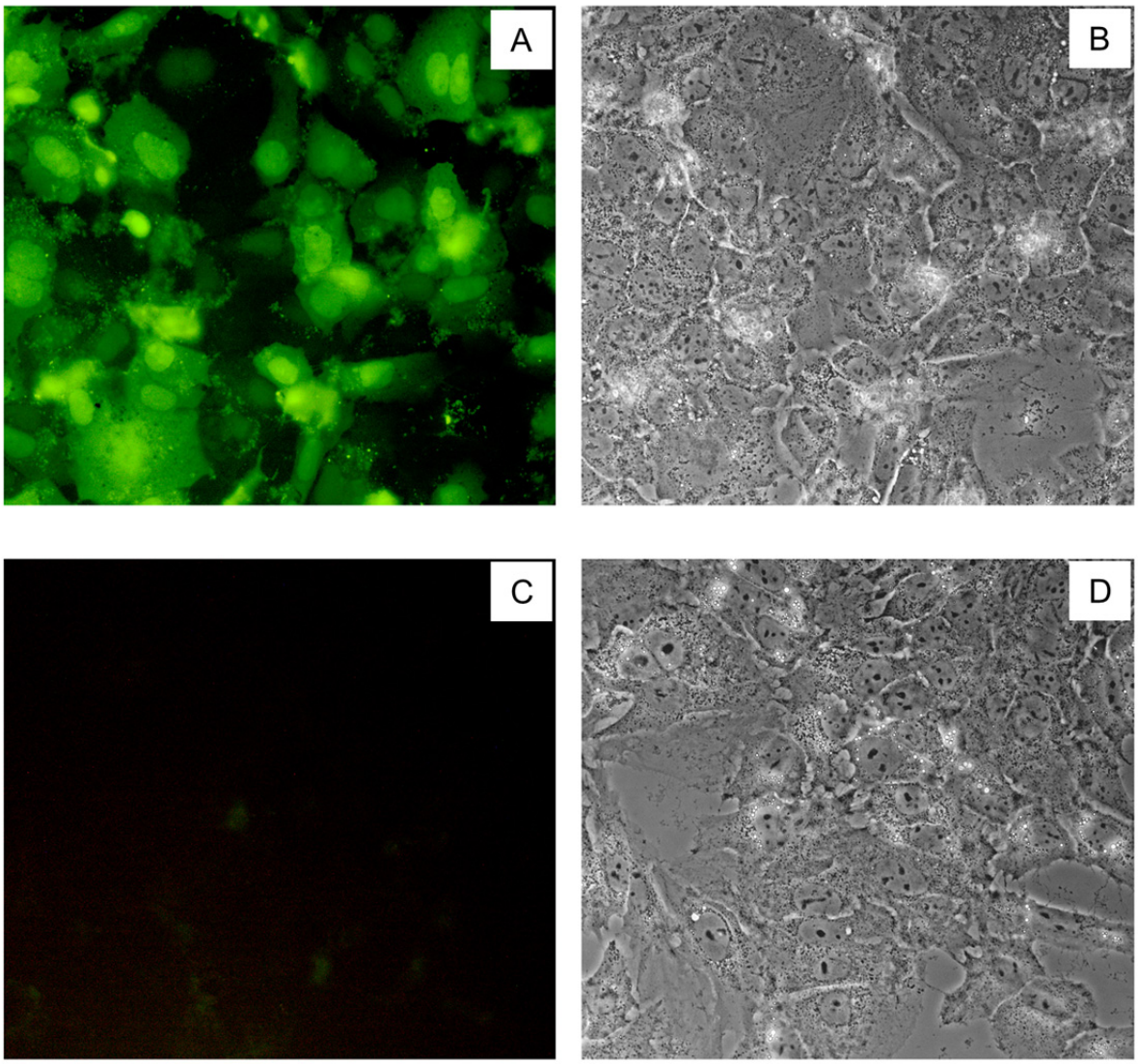

Figure 18. The HCV4 peptide enters huh-7.5 cells efficiently. Cells were treated with 500nM FITC-HCV4 and washed three times with PBS after 40 minutes and imaged. **A** and **C.** Fluorescent images of FITC-HCV4 treated and untreated cells, respectively. **B** and **D.** phase-contrast images of the same cells as in panels A and C, respectively.

to competitively block pull-down of NS5A domain I, while the HCV2 sequence scrambled control peptide (Table 1) did not (Figure 21A). To determine if the HCV4 peptide interacts with HSP70 *in vivo*, FITC-labeled HCV4 was introduced into huh-7.5 cells followed by immunoprecipitation with anti-FITC antibody or IgG isotype

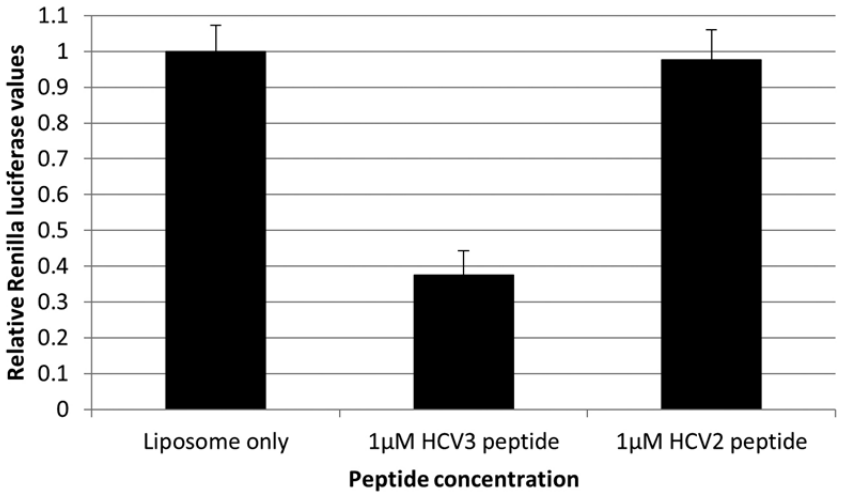

Figure 19. The HCV3 peptide corresponding to the C34 hairpin structure blocks viral protein production. Huh-7.5 cells were infected with the *Renilla* reporter virus and immediately treated with 1μM of HCV3 peptide or the HCV2 sequence-scrambled control peptide using liposomes. 24 hours post treatment, cells were harvested and assayed for *Renilla* luciferase activity. (Error bars reflect standard deviation.)

control. Western analysis demonstrated HCV4/HSP70 complex formation (Figure 21B).

2.2 Discussion

We and others have previously reported the NS5A/HSP70 interaction[33, 47]. However, direct interaction between NS5A and HSPs was not demonstrated due to the use of cellular systems. Here we report a direct interaction between NS5A and HSP70 using purified recombinant proteins and *in vitro* pull-down assays. This suggests that no other viral or cellular protein is necessary for the interaction between NS5A and HSP70.

Deletion studies of NS5A domain I narrowed down the HSP70-binding site to the C terminus of NS5A domain I (C34). Recently it was shown that NS5A amino acids 221-302 may be responsible for NS5A/HSP70 interaction[48]. This region

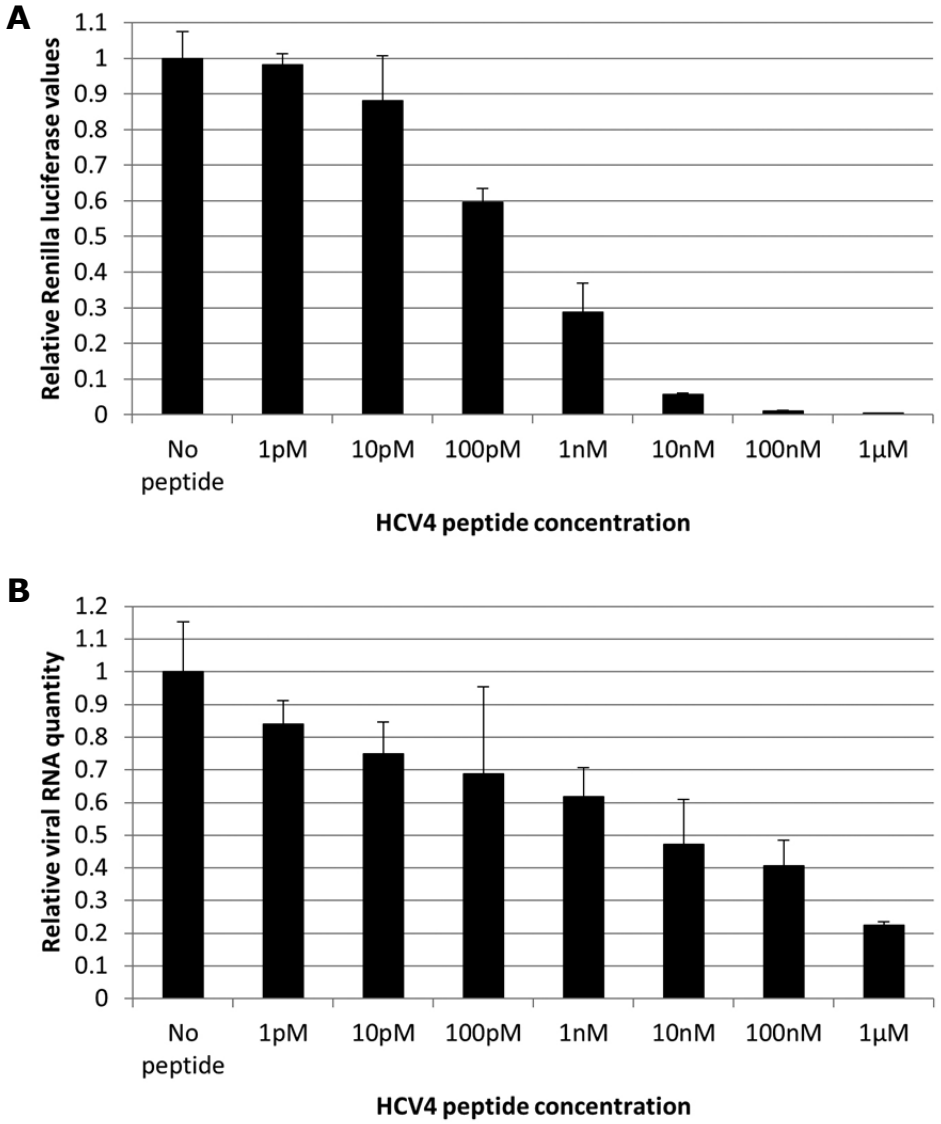

Figure 20. HCV4 peptide treatment inhibits infectious virion secretion and viral RNA replication. Huh-7.5 cells were treated with HCV4 and immediately infected with *Renilla* reporter virus. **A.** Forty-eight hours later, the supernatant was used to infect naïve cells. Forty-eight hours post infection, the cells were harvested and assayed for *Renilla* luciferase activity. **B.** Huh-7.5 cells were treated with HCV4 and infected as in part A. Forty-eight hours later, cell lysates were used to quantify viral RNA levels. (Error bars reflect standard deviation.)

includes most of the N terminus of NS5A domain II and some of the linker peptide between domains I and II. While this region does not directly bind HSP70, as shown by our *in vitro* interaction studies using purified proteins, it may represent an

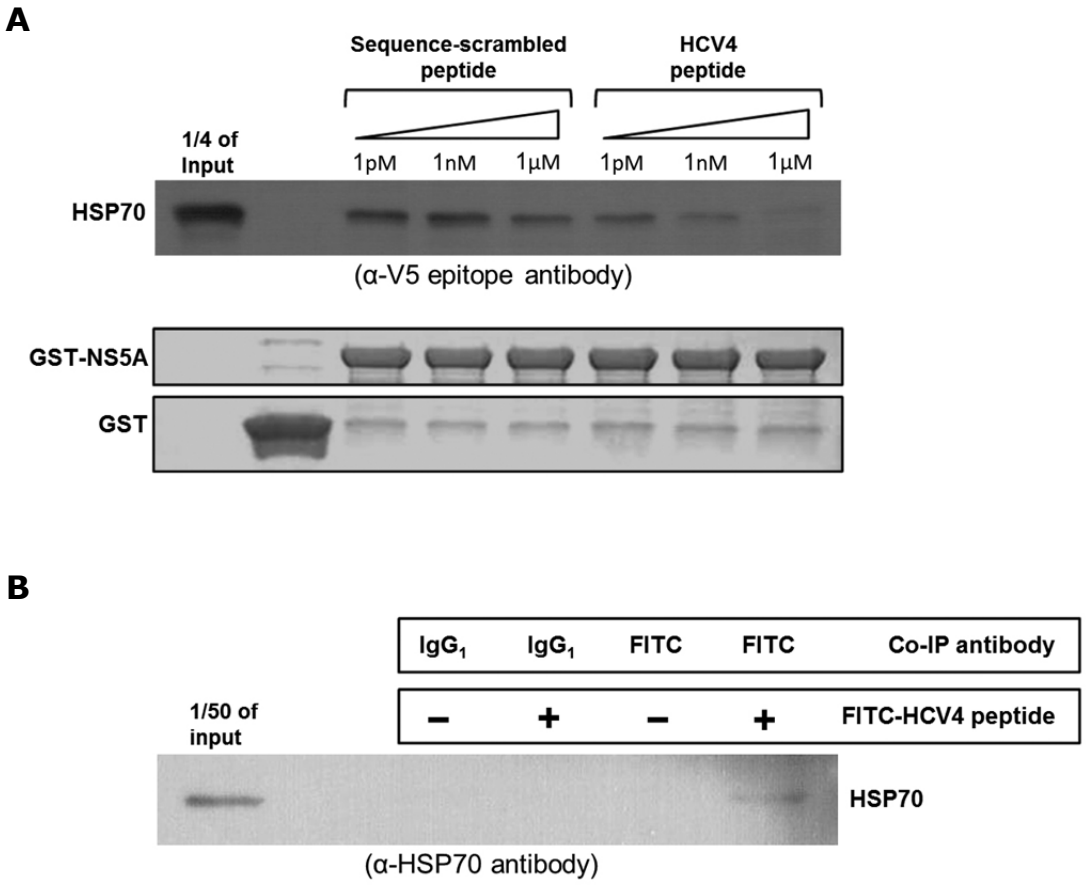

Figure 21. The HCV4 peptide blocks NS5A/HSP70 binding *in vitro* and binds HSP70 *in vivo*. **A.** GST pull-down assays showing that increasing concentrations of the HCV4 peptide competitively blocks pull-down of HSP70 with GST-NS5A while the sequence-scrambled control peptide (Table 1) does not. **B.** HSP70 co-immunoprecipitates with HCV4. Huh-7.5 cells were treated with 1μM FITC-HCV4 and harvested 24 hours later for co-immuno-precipitation (co-IP). Co-IP targets were analyzed through Western analysis with antibody against HSP70 demonstrating that the peptide binds HSP70 *in vivo*.

indirect interaction. In another report, a region of NS5A including the entire domain II and the first few amino acids of domain III was shown to inhibit NS5A-augmented IRES-mediated translation[28]. Both of these reports point to a common region in NS5A (i.e. domain II), and thus, it may be possible that NS5A domain II have a negative effect on IRES-mediated translation through (an) adaptor

protein(s). However, further biochemical studies are needed to verify (an) indirect interaction(s).

Our data shows that the C34 hairpin is the site of NS5A/HSP70 interaction. This is supported by the fact that the HCV4 peptide is able to block pull-down of HSP70 with NS5A *in vitro* as well as bind HSP70 *in vivo* (Figure 21). Furthermore, the C34 hairpin is the only region of C34 with a secondary structure, based on the crystal structure[34]. It has been reported that HSP27 also binds NS5A at residues 1-181[49]. It is important to note that the C34 hairpin structure lies exactly at the C terminus of this region. Thus, it may be possible that, in addition to HSP70, other HSPs either interact with the C34 hairpin or are also in complex with HSP70. Recently an alternate crystal structure of dimeric NS5A domain I was published which displays the two domain I units to be closer together closing the proposed RNA-binding cleft[50]. Analysis of this structure reveals the two C34 hairpins to be also exposed.

HSP70 binds non-specifically to a large number of hydrophobic peptide sequences (nascent or denatured) through its C-terminal substrate-binding domain (SBD) allowing the client peptide to attain its native conformation[32]. The N-terminal nucleotide binding domain (NBD) of HSP70 does not interact with peptides directly. Rather, it binds ATP and hydrolyzes it to ADP to induce conformational changes in SBD to facilitate its function[32]. NS5A hydrophobicity plot reveals that C34 is not significantly hydrophobic, and the C34 hairpin is, in fact, hydrophilic (Figure 22). Our findings reveal a specific and sequence-dependent interaction between HSP70 and NS5A as there are many regions in NS5A domain I as well as in other domains that are significantly more hydrophobic than C34. This specific interaction is further

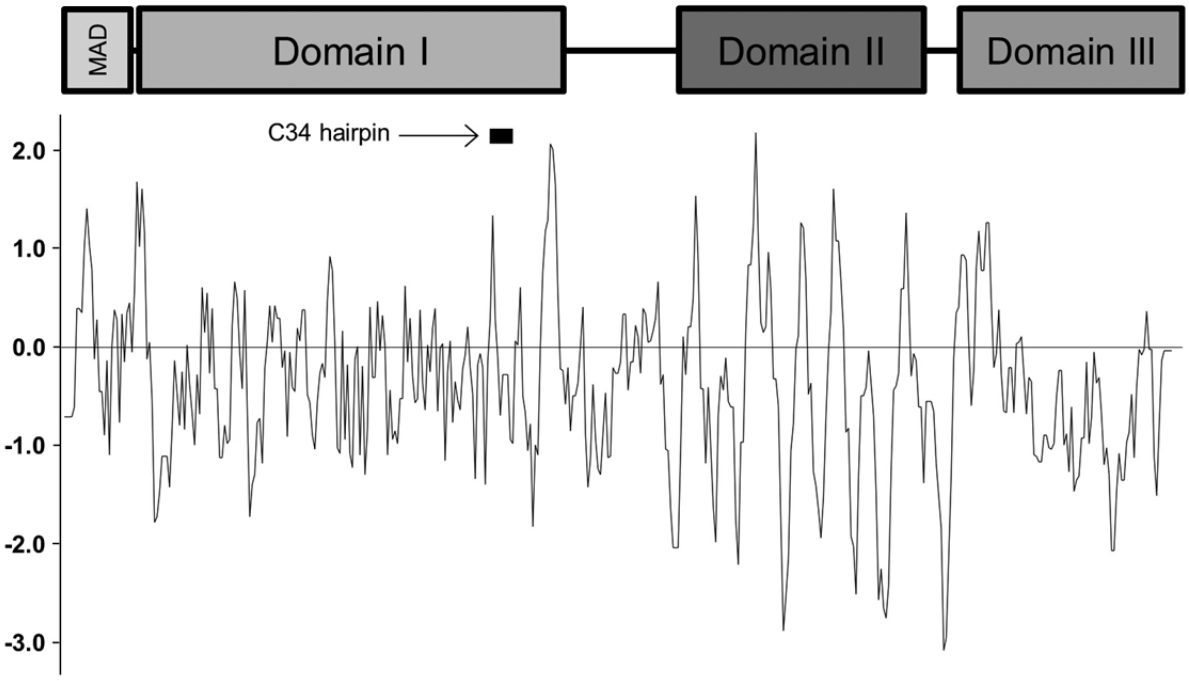

Figure 22. The hydrophobicity plot of NS5A. The plot is generated using the Kyte and Doolittle scale with a window size of seven. The location of C34 hairpin is indicated.

verified by our discovery that only HSP70-NBD binds NS5A directly. HSP70-NBD is known to interact with proteins that regulate the HSP70 chaperone activity. These proteins include BAG5, co-chaperones of J-domain proteins (such as HSP40), and HSP110 all of which bind HSP70-NBD[32, 51-53]. Thus, interactions with NBD of HSP70 are an important regulatory mechanism, and it may be possible that NS5A modulates HSP70 activity as well resulting in increased IRES activity.

NS5A domains II and III have been implicated in viral genome replication and virion assembly[15, 17], and domains I, II, and III have been shown to bind viral RNA[54]. None of the NS5A domains, however, have been previously ascribed to regulation of viral IRES-mediated translation. In this study, we have shown that NS5A domain I plays an important role in regulation of IRES-mediated translation

through the C34 beta-sheet hairpin structure. We have shown that C34 expression and treatment with the C34 hairpin peptide derivative (HCV4) block NS5A-augmented IRES-mediated translation. This effect is sequence specific as peptides of equal length from NS5A domains II and III fail to produce similar results. We have previously shown that Quercetin treatment and HSP70 knock-down block NS5A-augmented IRES-mediated translation[33]. Taken together, our data implicates the C34 hairpin of NS5A domain I in the regulation of viral IRES-mediated translation.

Our current model of NS5A-augmented IRES-mediated translation consists of a complex of NS5A, HSP70, HSP40, and probably additional, yet unidentified, factors such as the ribosome which may stabilize the translation complex (Figure 23). An RNA-binding cleft between the two claw-like domain I units has been predicted in the crystal structure[34] (Figure 15). It has also been reported that HSP70 (specifically the HSPA1A isoform used in this study) is able to bind to the 40S ribosomal subunit[55]. Our finding that NS5A directly binds HSP70, therefore, provides a possible link between the NS5A dimers and the ribosome both of which interact with the RNA template. This NS5A/HSP70 interaction may be responsible for stabilizing the components of translation machinery on the RNA template during translation initiation and/or elongation.

The significance of C34 region and the hairpin within is further underlined by the mutation analysis of HCV genome[44]. As shown in Figure 24, the majority of insertion mutants in C34 and all mutants within the hairpin are detrimental for the virus. Quite interestingly, mutation of the region immediately upstream of the hairpin and the region a few amino acids downstream are well tolerated (Figure

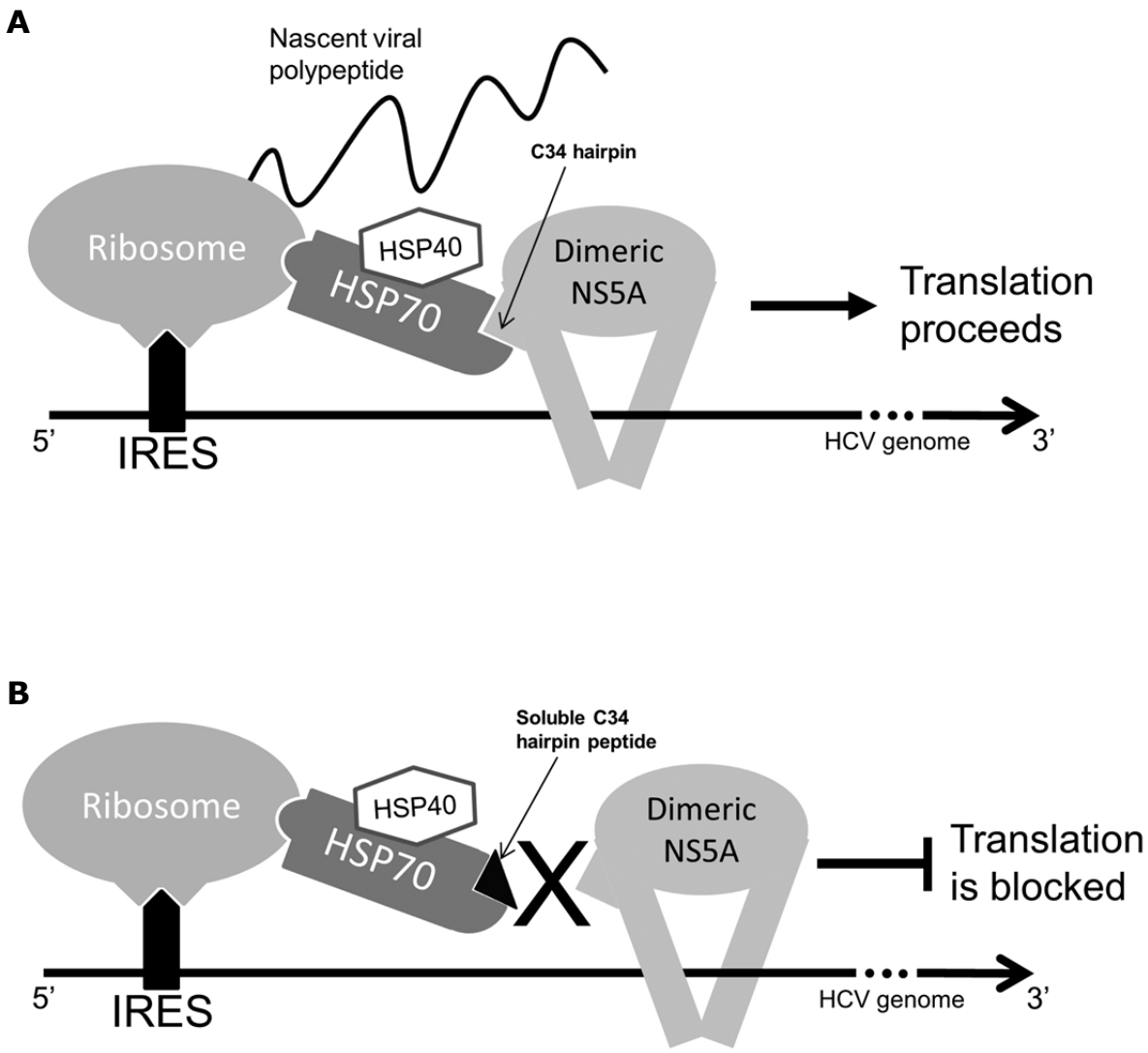

Figure 23. A proposed model of NS5A-augmented IRES-mediated translation. **A.** Our data supports the hypothesis that the NS5A/HSP70 complex formation is important for NS5A-augmented IRES-mediated translation. **B.** Soluble C34 hairpin peptide derivative inhibits NS5A/HSP70 binding resulting in the inhibition of NS5A-augmented IRES-mediated translation.

24). This data supports our hypothesis that the C34 hairpin is critical for viral proliferation.

It is known that in the context of chronic HCV infection, a number of viral proteins including NS5A are able to dramatically alter host gene expression to

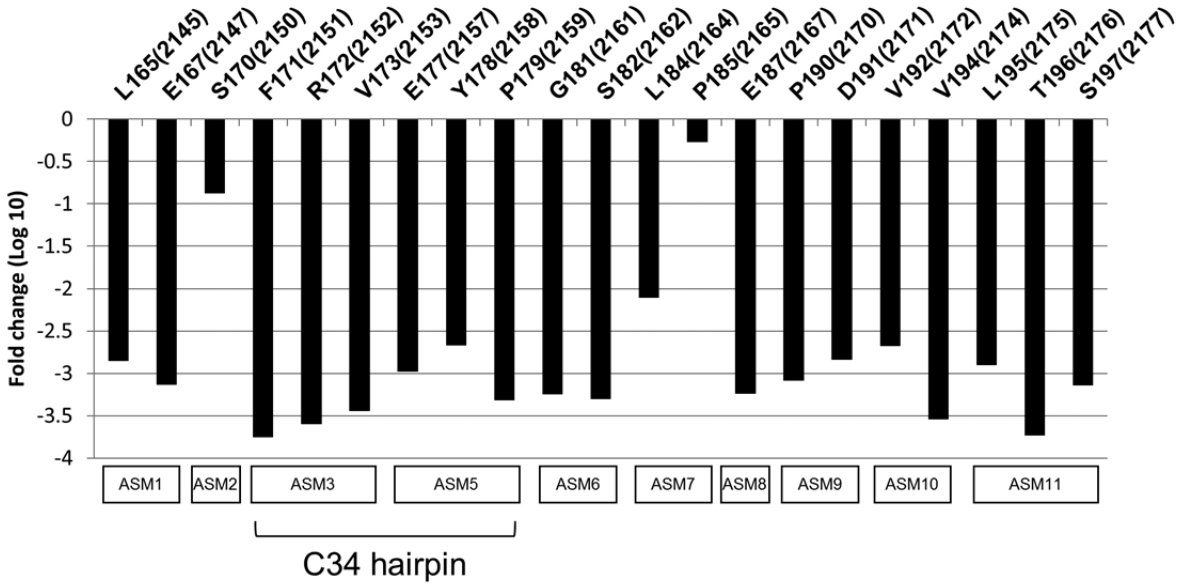

Figure 24. High resolution profile of 15 nucleotide insertion mutations of HCV genome across the C34 region. The figure is based on a previous report[43]. The amino acid positions of the alanine-scan mutants of Figure 14 are also indicated. Mutations immediately upstream and slightly downstream of C34 hairpin are well tolerated as opposed to other mutation in C34.

evade the innate immune response to viral infection resulting in the low efficacy of the currently available PEG-IFN and ribavirin treatment. Our findings demonstrate the significance of the NS5A/HSP70 interaction and the role of HSPs in HCV life cycle, in particular, IRES-mediated viral protein translation. Therefore, the C34 modified hairpin peptide may be a candidate for HCV therapy. Furthermore, considering the potency of the C34 hairpin peptide in suppressing viral translation levels, treatment with this peptide may significantly improve the efficacy of PEG-IFN and ribavirin treatment in patients resistant to these compounds or allow for IFN-free therapy in combination with other antiviral agents, which may be beneficial for patients unable to receive IFN therapy.

2.3 Materials and Methods

2.3.1 Plasmid constructs and cloning. All primers used for this study are obtained from Integrated DNA Technologies. All PCR products were gel-purified using QIAquick Gel Extraction Kit (Qiagen, cat. 28704). All restriction endonucleases were obtained from New England Biosciences (NEB). HSP70 and HSP40 were amplified from huh-7 cDNA using polymerase chain reaction (PCR), and NS5A was amplified from pMSCV-NS5A-FLAG described previously[33]. pGEX-6P-2 plasmid (Amersham, 28-9546-50) was used to generate N-terminal GST-fusion HSP70, HSP40, and NS5A as well as HSP70 nucleotide binding domain and substrate binding domain. The plasmid and the corresponding PCR products were double-digested with *Eco*RI and *Not*I restriction endonucleases. pET-28b plasmid (Novagen, 69865-3) was used to generate C-terminal His_6-tagged HSP70, HSP40, and NS5A. The plasmid and the corresponding PCR products were double-digested with *Eco*RI and *Not*I (for NS5A) and *NcoI* and *NotI* (For HSP70 and HSP40) restriction endonucleases. The pET-28b-NS5A construct was further subjected to site-directed mutagenesis in order to remove the sequence between the *Nco*I (which contains the ATG start codon) and *Eco*RI sites. This two-step strategy was necessary as NS5A itself contains an internal *Nco*I restriction site (refer to plasmid manual). pTRACER-EF/Bsd A plasmid (Invitrogen, V889-01) was used to generate C-terminal V5-epitope-tagged NS5A, HSP70, and HSP40 and all NS5A subclones. The plasmid and corresponding PCR products were double-digested with *Eco*RI and *Not*I restriction endonucleases. The C34 construct as well as the NS5A domain II and domain III peptides, the NS3 peptide (P19), and the C34 mutagenesis constructs (ASMs) were cloned into pCCL-CMV-IRES-EGFP plasmid. The peptide

PCR products and pCCL-CMV-IRES-EGFP were digested with *Eco*RI and *Nhe*I-HF restriction endonucleases. The integrity of all cloned constructs was verified through sequencing as well as diagnostic gel electrophoresis of digested plasmids. pRSET A plasmid (Invitrogen, V351-20) was used for generating C34 alanine mutants by site-directed mutagenesis as its smaller size compared with pCCL-CMV-IRES-EGFP allows for much more efficient mutagenesis. Two additional mutagenesis constructs were designed for ASM10 and ASM11 as alanine mutagenesis did not result in significant changes. Therefore, VAV and LTSM were mutated to SSS (M10) and SAGS (M11) for ASM10 and ASM11, respectively. All 13 mutagenized constructs were cloned into pCCL-CMV-IRES-EGFP as mentioned above. The HCV IRES reporter plasmid pNRLFC, and the GFP retroviral expression vector pMSCVGFP have been previously described[33].

2.3.2 Production and purification of recombinant proteins. GST-fusion proteins were expressed in bacteria and purified as previously described[56]. His_6-tagged proteins were expressed and purified using Ni-NTA Agarose bead slurry (Qiagen, 1018244) according to manufacturer's instructions. V5-epitope-tagged proteins were expressed using TNT T7 Coupled Reticulocyte Lysate System (Promega, L4610).

2.3.3 GST pull-down assays. GST pull-down assays were performed as previously described[56]. Pull-down targets were evaluated by western analysis.

2.3.4 Antibodies. HSP70 (Santa Cruz Biotech, C92F3A-5), HSP40 (Abcam, ab56589), NS5A (Abcam, ab20342), V5 epitope (Millipore, AB3792), and allophyco-cyanin-conjugated-anti-FLAG (PerkinElmer, AD0059F).

2.3.5 Cell culture. Cell lines 293T and huh-7.5 were maintained in a humidified atmosphere containing 5% CO_2 at 37°C in Dulbecco's Modified Eagle Medium (Mediatech, 10-013-CM) supplemented with 10% fetal bovine serum (Omega Scientific, FB-01) and 2 mM L-glutamine (Invitrogen, 25030).

2.3.6 IRES reporter assay. 293T cells were transfected with the HCV IRES reporter plasmid and either pMSCV-NS5A-FLAG (bearing wild-type NS5A or one of the mutants) or pMSCV-GFP. The pCCL-CMV-IRES-EGFP plasmid expressing one of the following peptides was also transfected where indicated: C34, NS5A domain II peptide, NS5A domain III peptide, NS3 peptide, or one of the C34 mutagenesis peptides. All transfections were done using Fugene6 (Roche, 11814443001). Forty-eight hours post transfection, *Renilla* and *Firefly* luciferase activity was determined using Dual Luciferase Assay System (Promega, E1910).

2.3.7 Flow cytometry. 293T cells were transfected with the construct expressing GFP, C34, NS5A domain II peptide, NS5A domain III peptide, or NS3 peptide. Forty-eight hours post transfection, the cells were harvested and analyzed by flow cytometry analysis for the FLAG fusion epitope. Cells were washed with PBS three times, fixed with 1.5% paraformaldehyde, and permeabilized with 0.05% nonidet p40. Cells were stained with 1:500 dilution of allophycocyanin-conjugated-anti-FLAG antibody for 30 minutes and washed three times with PBS. Flow cytometry was performed using Becton Dickinson FACSCalibur cytometer and Cellquest v3.3 software.

2.3.8 Infectious virus production. pNRLFC was *in vitro* transcribed, and the purified RNA was electroporated into huh-7.5 cells to generate infectious viral

supernatant as previously described[44]. Viral assays were done using the HCV reporter virus as described previously[33].

2.3.9 Crystal structure analysis. The figures representing crystal structure of NS5A domain I were generated by the PyMol software and '1ZH1' pdb file of dimeric NS5A domain I reported previously[34].

2.3.10 Peptide synthesis and characterization. Peptides were synthesized by the solid phase method using CEM Liberty automatic microwave peptide synthesizer (CEM Corporation), applying 9-fluorenylmethyloxycarbonyl (Fmoc) chemistry[57] and standard, commercially available amino acid derivatives and reagents (EMD Biosciences and Chem-Impex International). Rink Amide MBHA resin (EMD Biosciences) was used as a solid support. Peptides were cleaved from resin using modified reagent K (TFA 94% (v/v); phenol, 2% (w/v); water, 2% (v/v); TIS, 1% (v/v); EDT, 1% (v/v); 2 hours) and precipitated by addition of ice-cold diethyl ether. Reduced peptides were purified by preparative reverse-phase high performance liquid chromatography (RP-HPLC) to >95% homogeneity and their purity evaluated by matrix-assisted laser desorption ionization spectrometry (MALDI-MS) as well as by analytical RP-HPLC).

2.3.10.1 Disulfide bond formation: Peptides were dissolved at a final concentration of 0.25 mg/ml in 50% DMSO:H_2O and stirred overnight at room temperature. Subsequently peptides were lyophilized and re-purified on a preparative C18 SymmetryShield™ RP-HPLC column to >95% homogeneity. Their purity was evaluated by MALDI-MS as well as by analytical RP-HPLC.

2.3.10.2 Analytical RP-HPLC: Analytical RP-HPLC was performed on a Varian ProStar 210 HPLC system equipped with ProStar 325 Dual Wavelength UV-Vis

detector with wavelengths set at 220 nm and 280 nm (Varian Inc.). Mobile phases consisted of solvent A, 0.1% TFA in water, and solvent B, 0.1% TFA in acetonitrile. Analyses of peptides were performed with an analytical reversed-phase C18 SymmetryShield™ RP18 column, 4.6×250 mm, 5µm (Waters Corp.) applying linear gradient of solvent B from 0 to 100% over 100 min (flow rate: 1 ml/min).

2.3.11 Cell viability. Cell viability was determined using MTT Cell Proliferation assay (ATCC, 30-1010K).

2.3.12 Liposome-mediated peptide delivery. HCV2 and HCV3 peptides were delivered to cells using Coatsome El-01-A Anionic empty Liposomes (NOF Corp.). A 10:1 ratio of liposome to peptide was used.

2.3.13 Fluorescent microscopy. All images were taken by Olympus CKX41 fluorescent microscope via DP2-BSW v2.1.6207 software.

2.3.14 Quantitative reverse-transcriptase PCR. Huh-7.5 cells were treated with peptide and infected with *Renilla* reporter virus. Forty-eight hours post infection, cells were harvested, and total RNA was extracted using RNeasy Mini Kit (Qiagen, 74104). cDNA was synthesized using iScript cDNA Synthesis Kit (Bio-Rad, 1708891). qRT-PCR was performed using the Applied Biosystems 7500 Fast Real-Time PCR System with 2x SYBR Green Master Mix (Diagenode, GMO-SG2x-A300) in 25µL reactions. The real-time PCR cycling conditions were 50°C for 2 minutes and 95°C for 10 minutes, followed by 40 cycles at 95°C for 15 seconds, 60°C for 30 seconds and 72°C for 30 seconds each as well as a final dissociation stage of 95°C for 15 seconds and 60°C for 1 minute. Primers for viral genome were derived from the 5' NCR and were CTGGGTCCTTTCTTGGATAA and CCTATCAGGCAGTACCACA.

HCV RNA levels were normalized to the housekeeping gene actin using the primers CCAACCGCGAGAAGATGA and CCAGAGGCGTACAGGGATAG.

2.3.15 Co-immunoprecipitation. Huh-7.5 cells were treated with 1μM of fluorescein isothiocyanate (FITC)-labeled HCV4 peptide. Twenty-four hours later, cell lysates of FITC-HCV4 treated and control (untreated) cells were used in co-immunoprecipitation (co-IP) assays with antibody against FITC and IgG1 as control. Co-IPs were done using Protein G Plus-Agarose Immunoprecipitation Reagent (Santa Cruz Biotech, sc-2002) according to manufacturer's instructions.

2.3.16 Statistical analysis. Error bars reflect standard deviation. P values were determined by student t test.

Chapter 3

Optimization of an Antiviral Peptide that Inhibits Virus Specific Translation of the Hepatitis C Viral Genome

The HCV4 peptide described in chapter 2 is a potent small molecule inhibitor of virus specific NS5A-driven IRES-mediated translation of the viral genome and is also capable of disrupting the NS5A/HSP70 complex formation *in vitro*. After identifying the C34 hairpin region, which corresponds to the HCV4 peptide, we sought to further characterize the NS5A/HSP70 binding site and identify the specific amino acid residues involved in this interaction with the goal of generating peptides that are even more effective in blocking viral proliferation compared to the HCV4 peptide.

3.1 Results

The C34 hairpin peptide consists of ten amino acids that form a beta-sheet hairpin structure (Figure 15). In collaboration with Dr. Piotr Ruchala at UCLA, we compared the sequence of H77[35] and Con1[34] NS5As at the hairpin site and identified four conserved residues: Phe171, Val173, Tyr178, and Leu175 (positions are based on the H77 sequence) (Table 2). We generated a number of peptides with substitutions at these residues and tested their efficacy at blocking HCV proliferation (Table 2). Substitutions at Phe171 and Val173 improved the potency of the peptides compared with HCV4, whereas substitutions at Tyr178 decreased peptide efficacy. In addition, substitution of other non-conserved amino acids with arginines allowed for synthesizing smaller peptides that were still capable of cellular entry without an arginine tag, which is present on the original HCV4 peptide.

3.1.1 Four amino acid residues are conserved in the C34 hairpin.

Comparison of the H77[35] and Con1[34] NS5A sequences at the C34 hairpin locus revealed four conserved residues: Phe171, Val173, Tyr178, and Leu175 (Table 2). We hypothesized that these four residues may be critical for the NS5A/HSP70 interaction. A structural analysis of the hairpin region in the crystal structure of dimeric NS5A domain I[34] revealed that Phe171, Val173, and Tyr178 occur within and on one side of the plane of the two beta-sheets, while Leu175 extends on the opposite face and is located on the linker region between the two beta-sheets (Figure 25). The spatial orientation of Phe171, Val173, and Tyr178 supports their role in forming a binding interface that interacts with HSP70, while the Leu175 residue may play a stabilizing role in this interaction.

			Sequence														
H77 Amino Acid Position			169	170	171	172	173	174	175	176	177	178	179	180			
Peptide	Crystal Structure		Val	Thr	Phe	Leu	Val	Gly	Leu	Asn	Gln	Tyr	Leu	Val			Cyclisation ?
HCV1			Val	Ser	Phe	Arg	Val	Gly	Leu	His	Glu	Tyr	Pro	Val	-$CONH_2$		No
HCV2			Tyr	Phe	Val	Pro	His	Glu	Ser	Gly	Arg	Val	Val	Leu	-$CONH_2$		No
HCV3			Cys	Ser	Phe	Arg	Val	Gly	Leu	His	Glu	Tyr	Pro	Cys	-$CONH_2$		-S-S- Bridge
HCV4	R-(Ahx-R)$_6$-Ahx-Ahx-		Cys	Ser	Phe	Arg	Val	(D)Pro	Cha	His	Glu	Tyr	Pro	Cys	-$CONH_2$		-S-S- Bridge
HCV5		Arg	Cys	Arg	Phe	Arg	Val	(D)Pro	Cha	His	Arg	Tyr	Arg	Cys	Arg	-$CONH_2$	-S-S- Bridge
HCV6	Pal-Ahx-Ahx-	Arg	Cys	Arg	Phe	Arg	Val	(D)Pro	Cha	His	Arg	Tyr	Arg	Cys	Arg	-$CONH_2$	-S-S- Bridge
HCV7		Arg	Cys	Arg	Phe	Arg	Val	(D)Pro	Cha	His	Arg	Bip	Arg	Cys	Arg	-$CONH_2$	-S-S- Bridge
HCV8		Arg	Cys	Arg	Phe	Arg	Val	(D)Pro	Cha	His	Arg	Dpa	Arg	Cys	Arg	-$CONH_2$	-S-S- Bridge
HCV9		Arg	Cys	Arg	Phe	Arg	Chg	(D)Pro	Cha	His	Arg	Tyr	Arg	Cys	Arg	-$CONH_2$	-S-S- Bridge
HCV10		Arg	Cys	Arg	Phe	Arg	CystBu	(D)Pro	Cha	His	Arg	Tyr	Arg	Cys	Arg	-$CONH_2$	-S-S- Bridge
HCV11		Arg	Cys	Arg	^{1}Nal	Arg	Val	(D)Pro	Cha	His	Arg	Tyr	Arg	Cys	Arg	-$CONH_2$	-S-S- Bridge
HCV12		Arg	Cys	Arg	Dpa	Arg	Val	(D)Pro	Cha	His	Arg	Tyr	Arg	Cys	Arg	-$CONH_2$	-S-S- Bridge
HCV13		Arg	Cys	Arg	Trp	Arg	Val	(D)Pro	Cha	His	Arg	Dpa	Arg	Cys	Arg	-$CONH_2$	-S-S- Bridge
HCV14		Arg	Cys	Arg	^{2}Nal	Arg	Chg	(D)Pro	Cha	His	Arg	Bip	Arg	Cys	Arg	-$CONH_2$	-S-S- Bridge
HCV15			Cys	Arg	^{2}Nal	Arg	Val	(D)Pro	Cha	His	Arg	Tyr	Arg	Cys	-$CONH_2$		-S-S- Bridge
HCV15R			Cys^{SH}	Arg	^{2}Nal	Arg	Val	(D)Pro	Cha	His	Arg	Tyr	Arg	Cys^{SH}	-$CONH_2$		No / reduced form
HCV16			-Ac	Arg	^{2}Nal	Arg	Val	(D)Pro	Cha	His	Arg	Tyr	Arg	Cys^{S-}	-$CONH_2$		-S-CH_2- / Thioether
HCV17			-Ac	Arg	^{2}Nal	Arg	Val	(D)Pro	Cha	His	Arg	Tyr	Arg	NH-$CH_2CH_2CH_2CH_2$S-			-S-CH_2- / Thioether
HCV18			Cys	Arg	^{2}Nal	Arg	Chg	(D)Pro	Cha	His	Arg	Tyr	Arg	Cys	-$CONH_2$		-S-S- Bridge
HCV19			-Ac	Arg	^{2}Nal	Arg	Chg	(D)Pro	Cha	His	Arg	Tyr	Arg	NH-$CH_2CH_2CH_2CH_2$S-			-S-CH_2- / Thioether
polyArg tag	R-(Ahx-R)$_6$ -$CONH_2$																
HCV18RI			(D)Cys	(D)Arg	(D)Tyr	(D)Arg	(D)His	(D)Cha	(L)Pro	(D)Chg	(D)Arg	(D)^{2}Nal	(D)Arg	(D)Cys	-$CONH_2$		-S-S- Bridge

Table 2. Sequence and characterization of all peptides generated. The red marks indicate amino acid substitutions that resulted in peptides with better efficacy at blocking HCV proliferation compared to HCV4. Peptides marked in red demonstrate higher efficacy than HCV4 in blocking viral proliferation. (2Nal = 2-naphthylalanine; -Ac = acetate; Ahx = 6-amino-hexanoic acid; Bip = Biphenyl-alanine; Cha = (L)cyclohexylalanine; Chg = cyclohexyl-glycine; CysSH = reduced cysteine; CystBu = S-tertButyl-(L)-Cysteine; Dpa = 3,3'-diphenyl-alanine; Pal = palmitoic acid)

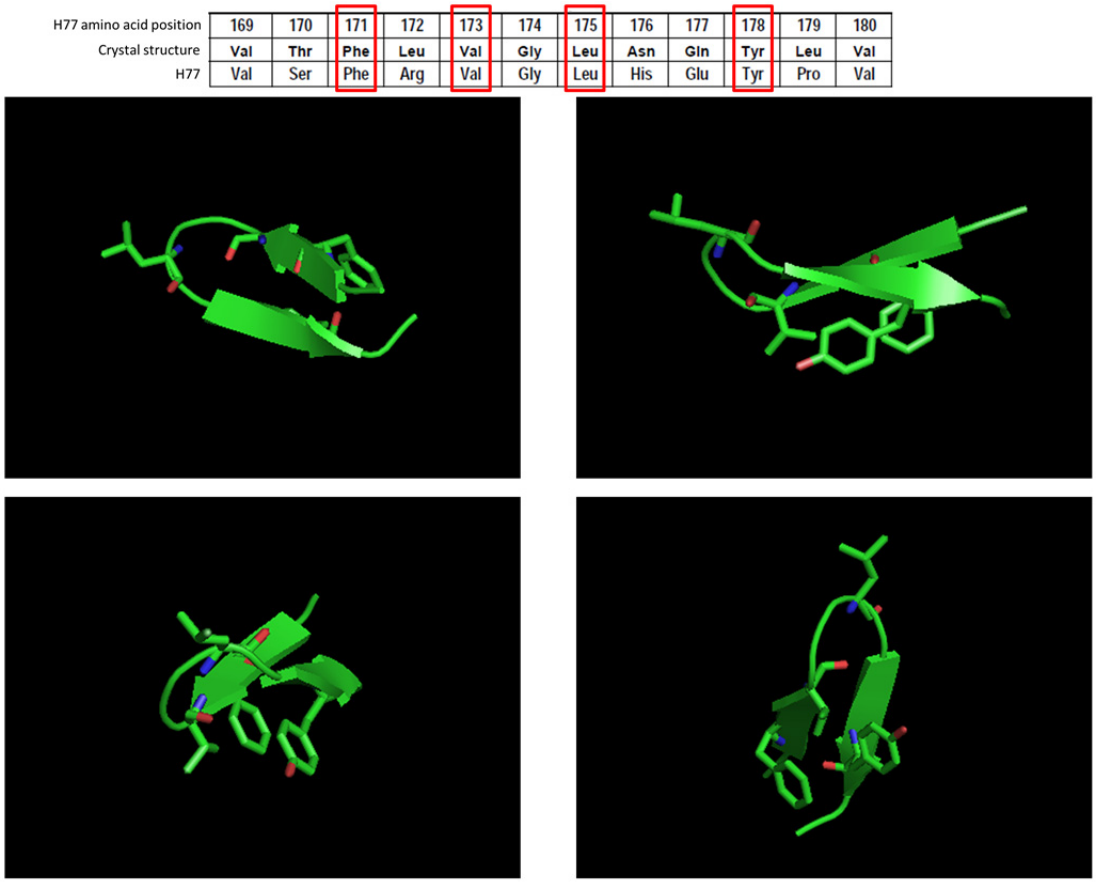

Figure 25. Schematics of the C34 hairpin region. The C34 hairpin region is shown at various angles. The four conserved residues are shown on all panels.

3.1.2 Substitutions at Phe171, Val173, and Tyr178 residues alter the activity of HCV4 derivative peptides. Based on the spatial arrangement of the Phe171, Val173, and Tyr178 residues, we hypothesized that substitutions within the synthetic hairpin peptides at these residues would affect their binding to HSP70 and, therefore, alter the antiviral activity of these peptides in the HCVcc infection system. Both Phe171 and Val173 residues have hydrophobic side chains, while the Tyr178 side chain is polar. All amino acid substitutions were intended to increase the hydrophobicity of these residues as they possess side chains with larger hydrophobic side chains. We synthesized a number of derivative peptides of HCV4

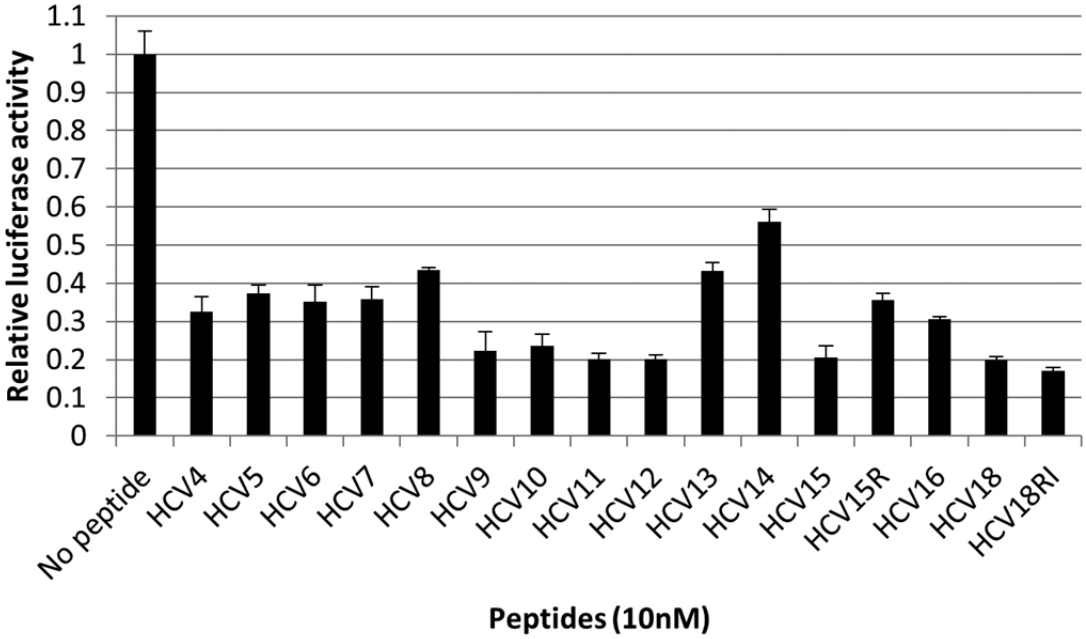

Figure 26. Modifications of the conserved amino acids within the C34 hairpin improves the anti-viral activity of the hairpin peptide. Refer to Table 2 for more details. Huh-7.5 cells were treated with peptides and immediately infected with reporter virus for three hours. Cells were assayed 24 hours post infection for *Renilla* activity. (Error bars reflect standard deviation.)

with substitutions at one, two, or all three residues and tested their efficacy at blocking HCV proliferation. We found that substitutions at either Phe171 or Val173 or both residues enhanced the antiviral activity of the peptides (Figure 26). This result indicates that increasing the hydrophobicity at these residues potentially enhances the binding of the peptide with HSP70. However, substitutions at the Tyr178 alone or in combination with Phe171 and/or Val173 decreased the efficacy of these peptides (Figure 26). This was expected as substitutions at Tyr178 eliminate the polarity of the side chain at this residue due to incorporation of hydrophobic amino acids, which may result in decreasing the binding capability of the peptide with HSP70.

3.1.3 Substitution of the non-conserved amino acids within the two beta-sheets of the hairpin maintains peptide antiviral activity and enables membrane penetration without an arginine tag. The HCV4 peptide consists of an arginine tag at its N terminus which allows for plasma membrane penetration. Addition of this tag significantly increases the molecular weight of the peptide and may lead to cellular toxicity. The two beta-sheets of the hairpin structure include four non-conserved residues: We hypothesized that these non-conserved residues can be substituted with arginines without significantly altering the antiviral activity of the peptides. As shown in Figure 26, these peptides maintained their antiviral activity compared to the HCV4 peptide, which indicates that they were capable of penetrating the plasma membrane. Furthermore, these peptides have the benefit of being smaller.

3.1.4 Cyclization of the peptides significantly improves their antiviral activity. We hypothesized that the characteristic anti-parallel beta sheet structure of the C34 hairpin may be important for the antiviral activity of the analog peptides. To test this hypothesis, we synthesized a non-cyclized (linear) analog of the HCV15 peptide with a reduced disulfide bond (HCV15R) and tested its antiviral activity along with the other peptides (Table 2). As shown in Figure 26, the linearization of the peptide significantly reduced its antiviral activity with the cyclized form being nearly twice as effective as the linear form. Linearization of the peptide may reduce the efficacy of the peptide by eliminating the optimal hairpin-like conformation of the peptide and/or decreasing its half-life as linear peptides may be more susceptible to enzymatic degradation.

3.1.5 Decreasing the length of the cyclizing linker in peptides decreases their antiviral activity. The majority of the peptide analogs used in this study are cyclized by a disulfide linker to achieve the hairpin-like structural conformation of the crystal structure (Figure 15). To determine if altering the length of the linker would affect the efficacy of the peptide, we synthesized an analog of the HCV15 peptide (HCV16) in which the disulfide linker is replaced by the shorter thioether linker by substituting the N-terminal cysteine with an acyl group (Table 2). Our infection assays demonstrate that decreasing the linker length negatively impacts the efficacy of the peptide (Figure 26). This may indicate that the binding of the C34 hairpin is highly optimized in the binding pocket such that shortening the linker pulls the hairpin beta sheets closer together thereby decreasing the peptide binding affinity.

3.2 Discussion

We have shown in the preceding chapter that the HCV4 peptide is a potent and dose-dependent inhibitor of HCV virus production. This peptide corresponds to the C34 hairpin moiety, which was identified by the deletion mutation analysis of the NS5A domain I and subsequent alanine scan mutagenesis of the C34 region (Chapter 2). Here we report a detailed structural analysis of the C34 hairpin region and synthesis of a panel of HCV4 analogs with enhanced anti-viral effects.

We identified four conserved amino acid residues in the hairpin region based on comparison of H77[35] and Con1[34] NS5A sequences (Table 2). The side chains of three residues (Phe171, Val173, and Tyr178) are oriented in one side of the plane of the two hairpin beta-sheets, while Leu175 extends on the opposite side and direction (Table 2 and Figure 25). We currently hypothesize that these residues are

involved in direct binding with HSP70 with Leu175 potentially acting as a binding stabilizer. Indeed substitution of Phe171, Val173, and Tyr178 with synthetic hydrophobic residues modulates the antiviral activity of the corresponding peptides. While Phe171 and/or Val173 substitutions enhance the efficacy of the peptides, substitution of the polar Tyr178 decreases the antiviral activity (Figure 26).

We also showed that cyclizing the peptides enhances their antiviral activity potentially by stabilizing the peptide conformation as a hairpin and/or minimizing the degradation of the peptides (Figure 26 and Table 2). Furthermore, shortening the cyclizing linker length from a disulfide to a thioether decreases the efficacy of the peptide indicating a highly optimized binding between HSP70 and NS5A in a tight binding pocket.

3.3 Materials and Methods

3.3.1 Crystal structure analysis. The figures representing crystal structure of NS5A domain I were generated by the PyMol software and '1ZH1' pdb file of dimeric NS5A domain I reported previously[34].

3.3.2 Peptide synthesis and characterization. Peptides were synthesized by the solid phase method using CEM Liberty automatic microwave peptide synthesizer (CEM Corporation), applying 9-fluorenylmethyloxycarbonyl (Fmoc) chemistry[57] and standard, commercially available amino acid derivatives and reagents (EMD Biosciences and Chem-Impex International). Rink Amide MBHA resin (EMD Biosciences) was used as a solid support. Peptides were cleaved from resin using modified reagent K (TFA 94% (v/v); phenol, 2% (w/v); water, 2% (v/v); TIS, 1% (v/v); EDT, 1% (v/v); 2 hours) and precipitated by addition of ice-cold diethyl ether. Reduced peptides were purified by preparative reverse-phase high

performance liquid chromatography (RP-HPLC) to >95% homogeneity and their purity evaluated by matrix-assisted laser desorption ionization spectrometry (MALDI-MS) as well as by analytical RP-HPLC).

3.3.2.1 Disulfide bond formation: Peptides were dissolved at a final concentration of 0.25 mg/ml in 50% DMSO:H_2O and stirred overnight at room temperature. Subsequently peptides were lyophilized and re-purified on a preparative C18 SymmetryShield™ RP-HPLC column to >95% homogeneity. Their purity was evaluated by MALDI-MS as well as by analytical RP-HPLC.

3.3.2.2 Analytical RP-HPLC: Analytical RP-HPLC was performed on a Varian ProStar 210 HPLC system equipped with ProStar 325 Dual Wavelength UV-Vis detector with wavelengths set at 220 nm and 280 nm (Varian Inc.). Mobile phases consisted of solvent A, 0.1% TFA in water, and solvent B, 0.1% TFA in acetonitrile. Analyses of peptides were performed with an analytical reversed-phase C18 SymmetryShield™ RP18 column, 4.6×250 mm, 5µm (Waters Corp.) applying linear gradient of solvent B from 0 to 100% over 100 min (flow rate: 1 ml/min).

3.3.3 Cell culture. The huh-7.5 cell line was maintained in a humidified atmosphere containing 5% CO_2 at 37°C in Dulbecco's Modified Eagle Medium (Mediatech, 10-013-CM) supplemented with 10% fetal bovine serum (Omega Scientific, FB-01) and 2 mM L-glutamine (Invitrogen, 25030). Huh-7.5 cells were a kind gift from Charles Rice (The Rockefeller University, New York, NY)[43].

3.3.4 Infectious virus production. pFNX-RLuc was *in vitro* transcribed, and the purified RNA was electroporated into huh-7.5 cells to generate infectious viral supernatant as previously described[44].

3.3.5 Viral assays. All viral assays were done using the HCV reporter virus and with the same titer and multiplicity of infection as described previously[33, 35].

3.3.6 Intracellular viral protein production. Huh-7.5 cells were infected for 3 hours and treated with peptides immediately after infection. Cells were harvested 24 hours later and luciferase activity was measured by the *Renilla* Luciferase Assay System (Promega, E2820).

Conclusion

This dissertation focuses on identifying novel inhibitors of HCV proliferation and elucidating the role of heat shock proteins (HSPs) in the HCV viral life cycle. We have previously identified a complex of HSP70 with NS5A and shown this complex formation to be important for the NS5A-augmented IRES-mediated translation of viral genome and virus production. In this report, we showed that the quercetin, an HSP synthesis inhibitor, and two other bioflavonoids structurally related to quercetin, catechin and naringenin, are capable of blocking HCV proliferation by different mechanisms. Quercetin was found to be a potent inhibitor of HSP70 induction, while catechin and naringenin had milder effect. Both catechin and naringenin displayed stronger inhibition of intracellular infectious virion assembly compared to quercetin. We also identified the site of NS5A/HSP70 interaction on NS5A to be a hairpin peptide of approx. 10 amino acids at the C terminus of NS5A domain I. The HCV4 peptide corresponding to this hairpin is able to dose-dependently block viral protein translation levels and virus production. Moreover, HCV4 dose-dependently blocks NS5A/HSP70 complex formation *in vitro* and is capable of pulling down HSP70 from cellular extracts. Finally we showed that three conserved residues within the hairpin form a binding interface with HSP70, and we were able to improve antiviral activity of the peptides by increasing the hydrophobicity of two of these residues. Thus, our results indicate that the NS5A/HSP70 complex formation is important for viral IRES-mediated translation and that disruption of this complex significantly inhibits virus production. Furthermore, our results show that quercetin, catechin, and naringenin may be used as potential therapeutics for HCV infection. In addition, the HCV4 peptide with

its approx. IC_{50} of 500pM is also a potentially potent therapeutic against HCV infection.

Bibliography

1. Shepard CW, Finelli L, Alter MJ. Global epidemiology of hepatitis C virus infection. The Lancet infectious diseases 2005;5:558-567.
2. El-Serag HB. Hepatocellular carcinoma: an epidemiologic view. Journal of clinical gastroenterology 2002;35:S72-78.
3. Gambarin-Gelwan M, Jacobson IM. Optimal dose of peginterferon and ribavirin for treatment of chronic hepatitis C. Journal of viral hepatitis 2008;15:623-633.
4. McHutchison JG, Patel K. Future therapy of hepatitis C. Hepatology 2002;36:S245-252.
5. El-Serag HB. Hepatocellular carcinoma: recent trends in the United States. Gastroenterology 2004;127:S27-34.
6. Butt AA, Skanderson M, McGinnis KA, Kwoh CK, Justice AC. Real-life Rates of treatment completion for HCV. Hepatology 2007;46:364A.
7. Falck-Ytter Y, Kale H, Mullen KD, Sarbah SA, Sorescu L, McCullough AJ. Surprisingly small effect of antiviral treatment in patients with hepatitis C. Annals of internal medicine 2002;136:288-292.
8. Ciesek S, Manns MP. Hepatitis in 2010: the dawn of a new era in HCV therapy. Nature reviews. Gastroenterology & hepatology 2011;8:69-71.
9. Baron S. Medical microbiology. 4th ed. Galveston, Tex.: University of Texas Medical Branch at Galveston, 1996: xvii, 1273 p.
10. Amako Y, Tsukiyama-Kohara K, Katsume A, Hirata Y, Sekiguchi S, Tobita Y, Hayashi Y, et al. Pathogenesis of hepatitis C virus infection in Tupaia belangeri. J Virol 2010;84:303-311.

11. Moradpour D, Penin F, Rice CM. Replication of hepatitis C virus. Nature reviews. Microbiology 2007;5:453-463.
12. Lindenbach BD, Rice CM. Unravelling hepatitis C virus replication from genome to function. Nature 2005;436:933-938.
13. Girard S, Vossman E, Misek DE, Podevin P, Hanash S, Brechot C, Beretta L. Hepatitis C virus NS5A-regulated gene expression and signaling revealed via microarray and comparative promoter analyses. Hepatology 2004;40:708-718.
14. Huang Y, Staschke K, De Francesco R, Tan SL. Phosphorylation of hepatitis C virus NS5A nonstructural protein: a new paradigm for phosphorylation-dependent viral RNA replication? Virology 2007;364:1-9.
15. Hughes M, Griffin S, Harris M. Domain III of NS5A contributes to both RNA replication and assembly of hepatitis C virus particles. The Journal of general virology 2009;90:1329-1334.
16. Reyes GR. The nonstructural NS5A protein of hepatitis C virus: an expanding, multifunctional role in enhancing hepatitis C virus pathogenesis. Journal of biomedical science 2002;9:187-197.
17. Tellinghuisen TL, Foss KL, Treadaway JC, Rice CM. Identification of residues required for RNA replication in domains II and III of the hepatitis C virus NS5A protein. Journal of virology 2008;82:1073-1083.
18. Appel N, Zayas M, Miller S, Krijnse-Locker J, Schaller T, Friebe P, Kallis S, et al. Essential role of domain III of nonstructural protein 5A for hepatitis C virus infectious particle assembly. PLoS pathogens 2008;4:e1000035.

19. Benga WJ, Krieger SE, Dimitrova M, Zeisel MB, Parnot M, Lupberger J, Hildt E, et al. Apolipoprotein E interacts with hepatitis C virus nonstructural protein 5A and determines assembly of infectious particles. Hepatology 2010;51:43-53.
20. Fridell RA, Qiu D, Valera L, Wang C, Rose RE, Gao M. Distinct Functions of NS5A in HCV RNA Replication Uncovered by Studies with the NS5A Inhibitor BMS-790052. Journal of virology 2011.
21. Peng L, Liang D, Tong W, Li J, Yuan Z. Hepatitis C virus NS5A activates the mammalian target of rapamycin (mTOR) pathway, contributing to cell survival by disrupting the interaction between FK506-binding protein 38 (FKBP38) and mTOR. The Journal of biological chemistry 2010;285:20870-20881.
22. Burckstummer T, Kriegs M, Lupberger J, Pauli EK, Schmittel S, Hildt E. Raf-1 kinase associates with Hepatitis C virus NS5A and regulates viral replication. FEBS letters 2006;580:575-580.
23. Kriegs M, Burckstummer T, Himmelsbach K, Bruns M, Frelin L, Ahlen G, Sallberg M, et al. The hepatitis C virus non-structural NS5A protein impairs both the innate and adaptive hepatic immune response in vivo. The Journal of biological chemistry 2009;284:28343-28351.
24. Wang C, Sarnow P, Siddiqui A. Translation of human hepatitis C virus RNA in cultured cells is mediated by an internal ribosome-binding mechanism. Journal of virology 1993;67:3338-3344.
25. Pacheco A, Martinez-Salas E. Insights into the biology of IRES elements through riboproteomic approaches. Journal of biomedicine & biotechnology 2010;2010:458927.

26. Spriggs KA, Stoneley M, Bushell M, Willis AE. Re-programming of translation following cell stress allows IRES-mediated translation to predominate. Biology of the cell / under the auspices of the European Cell Biology Organization 2008;100:27-38.
27. He Y, Yan W, Coito C, Li Y, Gale M, Jr., Katze MG. The regulation of hepatitis C virus (HCV) internal ribosome-entry site-mediated translation by HCV replicons and nonstructural proteins. The Journal of general virology 2003;84:535-543.
28. Kalliampakou KI, Kalamvoki M, Mavromara P. Hepatitis C virus (HCV) NS5A protein downregulates HCV IRES-dependent translation. The Journal of general virology 2005;86:1015-1025.
29. Vasconcelos DY, Cai XH, Oglesbee MJ. Constitutive overexpression of the major inducible 70 kDa heat shock protein mediates large plaque formation by measles virus. The Journal of general virology 1998;79 (Pt 9):2239-2247.
30. Weeks SA, Miller DJ. The heat shock protein 70 cochaperone YDJ1 is required for efficient membrane-specific flock house virus RNA replication complex assembly and function in Saccharomyces cerevisiae. Journal of virology 2008;82:2004-2012.
31. Zheng ZZ, Miao J, Zhao M, Tang M, Yeo AE, Yu H, Zhang J, et al. Role of heat-shock protein 90 in hepatitis E virus capsid trafficking. The Journal of general virology 2010;91:1728-1736.
32. Mayer MP, Bukau B. Hsp70 chaperones: cellular functions and molecular mechanism. Cellular and molecular life sciences : CMLS 2005;62:670-684.

33. Gonzalez O, Fontanes V, Raychaudhuri S, Loo R, Loo J, Arumugaswami V, Sun R, et al. The heat shock protein inhibitor Quercetin attenuates hepatitis C virus production. Hepatology 2009;50:1756-1764.
34. Tellinghuisen TL, Marcotrigiano J, Rice CM. Structure of the zinc-binding domain of an essential component of the hepatitis C virus replicase. Nature 2005;435:374-379.
35. Khachatoorian R, Arumugaswami V, Ruchala P, Raychaudhuri S, Maloney EM, Miao E, Dasgupta A, et al. A cell-permeable hairpin peptide inhibits hepatitis C viral nonstructural protein 5A-mediated translation and virus production. Hepatology 2012;55:1662-1672.
36. Khachatoorian R, Arumugaswami V, Raychaudhuri S, Yeh GK, Maloney EM, Wang J, Dasgupta A, et al. Divergent antiviral effects of bioflavonoids on the hepatitis C virus life cycle. Virology 2012;433:346-355.
37. Goldwasser J, Cohen PY, Lin W, Kitsberg D, Balaguer P, Polyak SJ, Chung RT, et al. Naringenin inhibits the assembly and long-term production of infectious hepatitis C virus particles through a PPAR-mediated mechanism. Journal of hepatology 2011;55:963-971.
38. Wellington K, Jarvis B. Silymarin: a review of its clinical properties in the management of hepatic disorders. BioDrugs 2001;15:465-489.
39. Wagoner J, Negash A, Kane OJ, Martinez LE, Nahmias Y, Bourne N, Owen DM, et al. Multiple effects of silymarin on the hepatitis C virus lifecycle. Hepatology 2010;51:1912-1921.

40. Elia G, Santoro MG. Regulation of heat shock protein synthesis by quercetin in human erythroleukaemia cells. The Biochemical journal 1994;300 (Pt 1):201-209.
41. Jakubowicz-Gil J, Pawlikowska-Pawlega B, Piersiak T, Pawelec J, Gawron A. Quercetin suppresses heat shock-induced nuclear translocation of Hsp72. Folia histochemica et cytobiologica / Polish Academy of Sciences, Polish Histochemical and Cytochemical Society 2005;43:123-128.
42. Li S, Kodama EN, Inoue Y, Tani H, Matsuura Y, Zhang J, Tanaka T, et al. Procyanidin B1 purified from Cinnamomi cortex suppresses hepatitis C virus replication. Antiviral chemistry & chemotherapy 2010;20:239-248.
43. Blight KJ, McKeating JA, Rice CM. Highly permissive cell lines for subgenomic and genomic hepatitis C virus RNA replication. J Virol 2002;76:13001-13014.
44. Arumugaswami V, Remenyi R, Kanagavel V, Sue EY, Ngoc Ho T, Liu C, Fontanes V, et al. High-resolution functional profiling of hepatitis C virus genome. PLoS pathogens 2008;4:e1000182.
45. Wegele H, Muller L, Buchner J. Hsp70 and Hsp90--a relay team for protein folding. Reviews of physiology, biochemistry and pharmacology 2004;151:1-44.
46. Gozdek A, Zhukov I, Polkowska A, Poznanski J, Stankiewicz-Drogon A, Pawlowicz JM, Zagorski-Ostoja W, et al. NS3 Peptide, a novel potent hepatitis C virus NS3 helicase inhibitor: its mechanism of action and antiviral activity in the replicon system. Antimicrobial agents and chemotherapy 2008;52:393-401.
47. Randall G, Panis M, Cooper JD, Tellinghuisen TL, Sukhodolets KE, Pfeffer S, Landthaler M, et al. Cellular cofactors affecting hepatitis C virus infection and

replication. Proceedings of the National Academy of Sciences of the United States of America 2007;104:12884-12889.

48. Chen YJ, Chen YH, Chow LP, Tsai YH, Chen PH, Huang CY, Chen WT, et al. Heat shock protein 72 is associated with the hepatitis C virus replicase complex and enhances viral RNA replication. The Journal of biological chemistry 2010;285:28183-28190.
49. Choi YW, Tan YJ, Lim SG, Hong W, Goh PY. Proteomic approach identifies HSP27 as an interacting partner of the hepatitis C virus NS5A protein. Biochemical and biophysical research communications 2004;318:514-519.
50. Love RA, Brodsky O, Hickey MJ, Wells PA, Cronin CN. Crystal structure of a novel dimeric form of NS5A domain I protein from hepatitis C virus. Journal of virology 2009;83:4395-4403.
51. Arakawa A, Handa N, Ohsawa N, Shida M, Kigawa T, Hayashi F, Shirouzu M, et al. The C-terminal BAG domain of BAG5 induces conformational changes of the Hsp70 nucleotide-binding domain for ADP-ATP exchange. Structure 2010;18:309-319.
52. Polier S, Dragovic Z, Hartl FU, Bracher A. Structural basis for the cooperation of Hsp70 and Hsp110 chaperones in protein folding. Cell 2008;133:1068-1079.
53. Vembar SS, Jin Y, Brodsky JL, Hendershot LM. The mammalian Hsp40 ERdj3 requires its Hsp70 interaction and substrate-binding properties to complement various yeast Hsp40-dependent functions. The Journal of biological chemistry 2009;284:32462-32471.

54. Foster TL, Belyaeva T, Stonehouse NJ, Pearson AR, Harris M. All three domains of the hepatitis C virus nonstructural NS5A protein contribute to RNA binding. Journal of virology 2010;84:9267-9277.
55. Cornivelli L, Zeidan Q, De Maio A. HSP70 interacts with ribosomal subunits of thermotolerant cells. Shock 2003;20:320-325.
56. French SW, Dawson DW, Chen HW, Rainey RN, Sievers SA, Balatoni CE, Wong L, et al. The TCL1 oncoprotein binds the RNase PH domains of the PNPase exoribonuclease without affecting its RNA degrading activity. Cancer letters 2007;248:198-210.
57. Fields GB, Noble RL. Solid phase peptide synthesis utilizing 9-fluorenylmethoxycarbonyl amino acids. International journal of peptide and protein research 1990;35:161-214.